A THEORETICAL INVESTIGATION AND EXPERIMENTAL VERIFICATION OF THE TWO-PHASE HEAT TRANSFER CHARACTERISTICS OF A COMBINED SOLAR COLLECTOR-GENERATOR FOR A SOLAR AIR CONDITIONER

By

GORDON LEE MOORE

A DISSERTATION PRESENTED TO THE GRADUATE COUNCIL OF
THE UNIVERSITY OF FLORIDA
IN PARTIAL FULFILLMENT OF THE REQUIREMENTS FOR THE
DEGREE OF DOCTOR OF PHILOSOPHY

UNIVERSITY OF FLORIDA

August, 1967

ACKNOWLEDGMENTS

The writer would like to express sincere appreciation for the timely encouragement and for the many helpful suggestions given by Dr. Erich A. Farber, chairman of the supervisory committee. The many hours of patient review of the research progress and the constructive criticism of the dissertation are hereby acknowledged.

Grateful appreciation is also due the members of the supervisory committee, Professors F. M. Flanigan, E. H. Hadlock, C. W. Pennington, and G. J. Schoessow, for their guidance in arranging the doctoral program and in its successful pursuit.

A special note of thanks is due Professor H. P. Patterson for his assistance and advice in material procurement policies.

The ready and able assistance of Dr. Richard Irey in the unending search for pertinent literature is greatly appreciated.

In the many essential operations requiring more than one pair of hands, the skillful assistance of Mr. Valimont Lansberry was invaluable. The informative and cheerfully given assistance of Mr. James Morris in the supply and maintenance of essential instrumentation is hereby acknowledged. The opportunity to draw upon the knowledge and experience of Mr. Richard Tomlinson was valued highly.

TABLE OF CONTENTS

LIST OF TABLES

LIST OF SYMBOLS

α	glass absorption coefficient
A	surface area
A_F	fin conduction area
A_L	liquid flow area
A_L'	tube surface wet by liquid
A_T	total circular tube flow area
A_V	vapor flow area
B	fin thickness
b	fin parameter $= \frac{U_L}{KB}$
c	specific heat
C_D	drag coefficient
C_P	specific heat at constant pressure
d, d_i	tube outside diameter, inside diameter
D	diameter
$D/d\tau$	substantial derivative
F	fin efficiency
F_D	drag force
F'	overall collection plate efficiency
g, g_c	acceleration due to gravity, gravitational constant
h_a, h_c	convective film coefficients
h_{fg}	heat of vaporization
h_r	coefficient of radiation and convective heat transfer

I	intensity of incident radiation
I_{DIR}	intensity of direct solar energy component
I_{DIFF}	intensity of diffuse solar energy
I_λ	monochromatic intensity
K	thermal conductivity, extinction coefficient
L	glass thickness
L'	length of refracted light beam
m	mass, mass flow rate
m_L, m_V	mass flow rate of liquid, vapor
n	index of refraction
P, P_L, P_V	pressure, liquid pressure, vapor pressure
P_e	Peclet number $= \frac{\bar{\omega} D}{\alpha}$
$Q, \bar{q}$	heat transfer rate, mean heat transfer rate
Q_A	heat collection rate per unit area
Q_{ABS}	heat out of absorber
Q_{COND}	heat out of condenser
Q_{EVAP}	heat into evaporator
Q_c	heat collected
Q_{GEN}	heat into generator
$Q_{u-PLATE}$	radiant heat to plate
$Q_{u-TUBES}$	radiant heat to tubes
Q_{u-x}	heat collection rate at X
π	glass surface reflectivity
R, R_i	radius, tube inside radius
Re_B	bubble Reynolds number
R_V	gas constant for the vapor

S	entropy, shade factor
T_A	air temperature
T_{EVAP}	evaporator
T_{GEN}	generator temperature
T_p, T_t	plate, tube temperature
T_{SAT}	saturation temperature
T_v, T_w	vapor, wall surface temperature
T_1	entrance temperature
u	internal energy
U_c	tube bond conductivity
U_L	overall heat loss coefficient
V, V_v	volume, vapor volume
$\bar{V}, \bar{V}_L, \bar{V}_v$	velocity, liquid velocity, vapor velocity
W	center to center tube spacing, width
α	absorptivity, diffusivity, angle
α_s	tube-sheet surface absorptivity
β	product solution parameter, angle
ϵ	emissivity, product solution variable
$\theta, \theta', \theta''$	angle of incidence, reflection, refraction
μ, μ_L	viscosity, liquid viscosity, microns
ρ, ρ_L, ρ_v	density, liquid density, vapor density
σ	surface tension
τ, τ_λ	transmissivity, monochromatic transmissivity
τ_i	shear at liquid vapor interface
τ_{w_v}	shear at wall surface contacting vapor flow

τ_{w_L}	shear at wall surface wet by liquid
μ	viscosity
ϕ	angle of inclination above horizontal
X	dimensionless coordinates
ψ	product solution variable
$\omega, \vec{\omega}, \bar{\omega}$	velocity, velocity vector, average velocity

Abstract of Dissertation Presented to the Graduate Council in Partial Fulfillment of the Requirements for the Degree of Doctor of Philosophy

A THEORETICAL INVESTIGATION AND EXPERIMENTAL VERIFICATION OF THE TWO-PHASE HEAT TRANSFER CHARACTERISTICS OF A COMBINED SOLAR COLLECTOR-GENERATOR FOR A SOLAR AIR CONDITIONER

By

Gordon Lee Moore

August, 1967

Chairman: Dr. Erich A. Farber

Major Department: Mechanical Engineering

Previous studies of solar refrigeration and air conditioning systems by other investigators have indicated that, when a conventional solar energy collector is used as the heat source in an absorption refrigeration system, an appreciable heat loss occurs in the transport of the heated fluid from the solar collector to the ammonia generator.

In the interest of reducing or eliminating this heat loss, a theoretical study was made of the various possible configurations which could serve the dual role of both a solar collector and an ammonia generator.

The combining of the solar collector and the ammonia generator into a single unit posed several problems involving the heat transfer and flow characteristics of the special geometric configurations making up the combined collector-generator.

In the theoretical analysis of the combined collector-generator, the incident solar energy is traced through each of the following phases:

1. Transmission through the glass cover of the collector-generator, to the tube sheet, through the tube sheet, and to the refrigerant fluid in the collector-generator tubes.

2. Two-phase effects appearing as
   a. Bubble growth and motion in the tubes.
   b. The vapor fraction and its effect on the heat transfer through the tube walls.

3. Final emergence as the heat of vaporization of ammonia vapor travelling from the collector-generator header to the condenser of the associated refrigeration system.

Utilizing information gained in the theoretical analysis, an experimental collector was designed and built using the following criteria:

1. Reasonable material and construction cost per unit of heat absorbed by the collector-generator per unit area.

2. Resistance to highly corrosive ammonia-water mixtures and safe withstanding of the working pressures involved.

3. Favorable flow of the two-phase mixtures in the passages where both phases appear.

4. Satisfactory separation of the two phases at strategic points in the complete refrigeration system.

Upon completion of the collector-generator unit, the condenser, evaporator, and absorber for an associated absorption refrigeration system were each designed, built, and added, one by one, to the refrigeration system. At each

stage of assembly of the various components into the system, a series of performance checks were made to determine the response of each successive system to solar energy input.

The first series measured the temperature response of the solar collector-generator alone under day long operation in full sunlight.

The second series utilized the collector-generator and the condenser as a "one-shot", intermittent refrigeration system.

The third and final series measured the performance of the collector functioning as a part of the complete absorption refrigeration system.

The theoretical analysis of the combined solar collector-generator and the results of the series of experimental investigations indicated the following advantages resulting from the combining of the two units into one:

1. The undesirable heat loss that occurs between solar collector and the separate generator of previous solar refrigeration systems is eliminated in the combined collector-generator.

2. The flat plate type solar collector generator can generate substantial amounts of ammonia even on cloudy days when only diffuse solar energy is available.

3. The solar collector-generator developed in this investigation can generate the equivalent of 30 pounds of ice per day with only a 4 by 4 foot collector area.

4. The combined collector-generator has a relatively short warm-up time.

CHAPTER I

INTRODUCTION

Previous investigations of solar driven absorption refrigeration systems have revealed a substantial and undesirable heat loss occurring in the heated liquid transport from the solar energy collector to the ammonia generator. In the interest of reducing or eliminating this loss, several investigators have proposed the combining of the solar collector and the ammonia generator into one unit.

The main purpose of this investigation has been to analyze theoretically the characteristics of such a combined system and then to design, construct, and operate the combined unit in a complete refrigeration system. However, an effort was also made to compact the entire system into a relatively small space. This reduction in size also resulted in a decrease in weight and cost of the system, thus bringing solar refrigeration closer to economic competition with existing, conventional systems. This effort to decrease the cost has a worthy end, since there is a great need in the world for a low-cost means of food preservation.

In recent National and International meetings on Solar Energy Utilization, it has been repeatedly emphasized

that much of the famine that now occurs in the world could be prevented if a low-cost means could be found for carrying over the abundance of one season into the season of scarcity. It has been stated that in some tropical countries, fully one-quarter of the vegetable crop spoils for lack of cooling facilities [1]. Also, it has been stated that factories in India can never operate at the efficiency of factories in the United States or Europe until they are air-conditioned [2]. Thus, the health of millions of people could be improved by the development of a low-cost cooling method.

For many of the underdeveloped countries of the world, solar refrigeration holds great promise as a solution to this problem, since most of the countries with this need have an abundance of sunshine. Also, this abundance comes at the season when refrigeration is most needed.

Thus, it can be seen that the basic research involved in this solar energy research project is not only of current scientific interest, but also has a world-wide economic significance.

CHAPTER II

PREVIOUS INVESTIGATIONS

Solar Refrigeration Studies at the University of Florida

The pioneer research in solar refrigeration began at the University of Florida in 1957, preceded by basic studies dating back to 1936, involving steam jet refrigeration [3] , mechanical refrigeration, and solar steam generation.

In 1957, a parabolic collector, 6 by 8 feet in size was built at the University's Solar Energy Laboratory. This collector focussed the sun's energy onto a glass covered tube at the focal line. The system followed the sun and heated oil to 550° F. This hot oil was stored and then circulated as needed to operate a standard Servel absorption refrigerator, providing the equivalent of domestic refrigeration. This system was technically feasible, but was not considered practical because of high construction and installation expenses [4] .

This study, however, did point to the use of a non-concentrating solar collector. Besides being less costly to build and easier to maintain and operate, the flat plate type collector intercepts both direct and diffuse radiation

and can collect considerable solar energy even on a cloudy day. As contrasted to the generating temperatures of conventional absorption refrigeration systems, the temperatures available from flat plate collectors are lower. Therefore, different refrigeration characteristics are needed when flat plate collectors are used. As a consequence, in 1957, a study was made of over 200 refrigerant combinations. The results of the study indicated that ammonia-water of about 60 per cent ammonia by weight offered the best overall properties for solar operated refrigeration and air-conditioning systems.

In 1958, a half-ton, intermittent ammonia-water system was built and found to operate satisfactorily [5]. This system required about 15 minutes charging time for each 45 minutes of cooling.

The next logical step was to try a continuous system. A three and one-half ton system was designed, built, and tested in 1962 and 1963 [6,7]. Although this system performed satisfactorily, it proved to be too large and expensive to compete with conventional systems.

Solar Refrigeration Studies at Other Institutions

Although refrigeration research began in the middle 1800's, interest in solar refrigeration has been relatively recent.

In 1956, F. Trombe [8], experimenting in France,

used a solar concentrator to operate an intermittent refrigeration device consisting of two small containers connected by a pipe. Refrigerant evaporating from one container was condensed in the other during the charging operation. When the operation was reversed, a cooling effect was obtained. This device was similar to an invention of the Crosley Corporation in 1920, called the "Icyball."

Williams et al. [9], at the University of Wisconsin, reported in 1958 the results obtained with a solar heated intermittent system similar to that of Trombe described above.

During 1960-61, Kapur [10], in India, and Tabor [11], in Israel, gave extensive surveys of the state-of-the-art in solar cooling.

In 1961 and 1962, Chinappa [12,13] reported on tests in India with a flat plate collector driving an ammonia-water absorption refrigeration system.

In 1962, Chung et al. [14], at the University of Wisconsin, gave the results of tests with a lithium bromide-water absorption air-conditioning system, using steam heat to simulate solar heat, but utilizing temperatures above those normally available from flat plate solar collectors. Also, it should be noted that the lithium bromide-water system used is capable of air-conditioning only, since this type system cannot produce temperatures low enough for refrigeration.

CHAPTER III

PURPOSE AND SCOPE OF THE PRESENT INVESTIGATION

Since it has been pointed out by previous investigators that there is a considerable heat loss between the solar collector and the generator of a solar driven refrigeration system, the next step in the development of a technically and economically more practical solar refrigeration system is believed to be the combining of the solar collector and the ammonia generator into one and the same unit. This poses a number of problems which seem not to have been answered in the literature. These problems involve the characteristics of varying concentrations of ammonia solutions as to flow and heat transfer, and changes which occur when some of the ammonia is driven out of solution, producing two-phase flow in the special geometric configurations involved in a combined solar collector-generator. In order to solve these problems, the following essential information is needed:

1. The theory of ammonia vapor production, two-phase flow, and separation characteristics in the special configurations involved.

2. The theoretical behavior of such mixtures in inclined flow systems.

3. Having established and verified the basic theoretical behavior, the design and development of such a combined system.

4. The actual performance characteristics of the resulting solar collector-generator in an operating solar refrigeration and air-conditioning system.

CHAPTER IV

THEORY

Introduction

The solar collector-generator developed in this investigation is similar to other flat plate solar collectors. The main difference is that the tubes are oriented in an up and down parallel pattern in the plane of the collector instead of being horizontal as is the case in most conventional collectors.

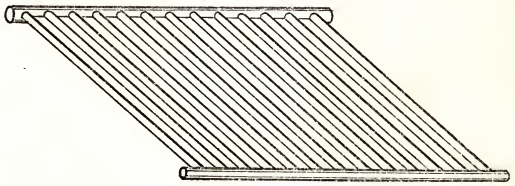

Figure 1

As is shown in Figure 1, the tubes terminate at headers at the upper and lower ends. These tubes will contain refrigerant fluid at gage pressures ranging from about 30 to 170 pounds per square inch.

This grid of parallel tubes is enclosed in a shallow, glass covered box-like structure and is inclined so that the glass covered face will be approximately normal to the sun's rays at solar noon during the summer season.

In order that solar radiation will be absorbed inside the enclosure, the tubes are bonded to a metal backing sheet and painted with a highly absorptive coating. The rear side of the enclosure is insulated to reduce heat losses from the heated metal sheet.

To analyze the various heat transfer phenomena that occur in this collector-generator, the energy in the incident solar radiation is traced from the point of its first striking the cover glass, through the cover glass, to the tube sheet, to the tubes, through the tube walls to the refrigerant flowing in the collector-generator tubes, and finally emerging in the form of the latent heat of ammonia vapor proceeding toward the condenser of the associated refrigeration system.

This analysis will be divided into the following steps:

1. Transmission through the collector-generator glass cover.
2. Transmission to the tube sheet.
3. Transmission through the tube sheet.
4. Transmission to the refrigerant fluid in the single-phase region.
5. Bubble growth and motion in the collector-generator tubes.
6. The effect of the vapor fraction on the two-phase heat transfer in the inclined collector-generator tubes.
7. The theory of operation of the complete solar driven refrigeration system.

Transmission Through the Collector-Generator Glass Cover

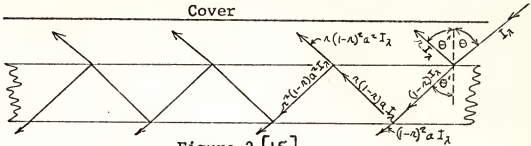

Figure 2 [15]

Part of the incident radiation is reflected by the upper surface of the cover glass, the remainder passing into the glass. This transmitted portion of energy is partially absorbed on its way through the glass, and upon reaching the lower surface of the glass is again separated into two parts. A small portion is reflected back upward into the interior and the remainder emerges through the lower surface as transmitted energy. That part of the energy which was reflected upward internally is, in turn, partially absorbed, reflected, or transmitted, etc. Because of this repeating pattern of successive absorption, transmission, and reflection, and because the re-reflection and consequent absorption quickly damps out, the total monochromatic transmissivity can be expressed as a converging, infinite series [16].

$$\tau_\lambda = (1-\rho)^2\alpha + \rho^2(1-\rho)^2\alpha^3 + \rho^4(1-\rho)^2\alpha^5 + \cdots$$

Since this is a geometric series, the sum is

$$\tau_\lambda = \frac{(1-\rho)^2\alpha}{1-\rho^2\alpha} .$$

This expression for τ_λ gives the fraction of incident radiation that finally emerges from the lower side of the collector-generator cover and proceeds toward the collector tube-sheet.

To evaluate α, the absorption coefficient, assume that the radiation absorbed in the cover glass is proportional to the length of the refracted beam L' and to the intensity of the incident radiation I_λ, or

$$\frac{dI_\lambda}{dL'} = K I_\lambda .$$

By definition, α is the ratio of two successive I_λ values. Integrating the above equation and taking the ratio of two successive values,

$$\alpha = \frac{I_{\lambda,2}}{I_{\lambda,1}} = e^{-KL'} .$$

For a given glass thickness L, due to the geometry of refraction by a glass with an index of refraction n,

$$L' = \frac{L}{\sqrt{1 - \frac{\sin^2\theta}{n^2}}} .$$

Typical values of K (the "extinction coefficient") are $0.174/_{IN}$ for 1/4 inch plate glass and $0.194/_{IN}$ for double strength window glass such as that used to cover the solar collector-generator [17].

To evaluate π the component reflectivity, a method developed by Valasek [18] is used. If it is

assumed that the normal and parallel components of the vibrations of the incident light beam are of equal intensity in the Fresnel relations, the value of π becomes

$$\pi = \frac{1}{2} \frac{\sin^2(\theta - \theta')}{\sin^2(\theta + \theta')} + \frac{\tan^2(\theta - \theta')}{\tan^2(\theta + \theta')}.$$

Note that, in all the above expressions for the net energy through the glass, there is a definite angular dependence. Thus, with the sun undergoing its diurnal motion, the energy transmitted through the glass cover of the collector-generator will never be constant, approaching a peak rate at solar noon and gradually diminishing in value from that point on.

Of the total solar energy that originally impinged upon the cover glass, about 10 per cent is finally absorbed by the glass, and the remainder proceeds on toward the collector plate or tube sheet. That portion of the incident energy that is absorbed by the cover glass serves to raise the temperature of the glass to some equilibrium value at which the energy leaves in the form of radiation and convection to the surroundings. Under operating conditions the net heat transfer will be upwards, since the glass is cooler than the tube sheet.

Now consider the net energy that has entered the glass covered enclosure and travels to the tube sheet.

Transmission to the Tube Sheet

A small fraction of the radiant energy which finally reaches the tube sheet surface is reflected upward by any non-blackness of this surface. The remainder of the energy is absorbed by the tube sheet and from there can follow any of three possible paths:

1. Most of the absorbed energy will be conducted through the tube walls to the refrigerant fluid.
2. Some of the energy will be lost by radiation and convection upward to the cover glass.
3. A small portion of energy will be lost by conduction through the edges and back of the collector-generator enclosure.

Since the tube sheet is at a relatively low radiation temperature (200° F or less), it is considered a low temperature emitter and all but a very minute fraction of its radiation will be in the far infra-red range of wave lengths. Since the commercial, double strength glass used to cover the collector-generator is practically opaque to all wave lengths of radiant energy greater than 2 or 3 microns, the radiant energy travelling upward from the tube sheet is effectively trapped by the glass cover. This phenomenon shown in Figure 3 is called the "Greenhouse Effect."

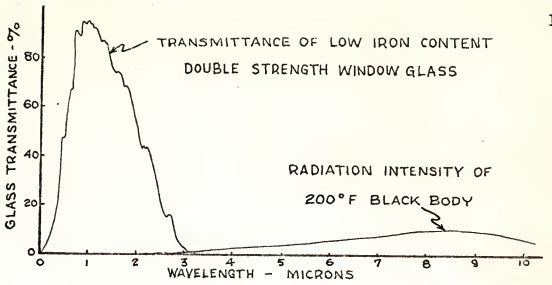

Figure 3

The amount of energy finally absorbed by the collector plate is

$$Q_{ABS} = \tau_G \alpha_S \left[(1-S) I_{DIR} + I_{DIFF} \right] .$$

The $(1-S)$ factor accounts for the fraction of oblique solar rays intercepted by the sides of the collector enclosure, as shown in Figure 4.

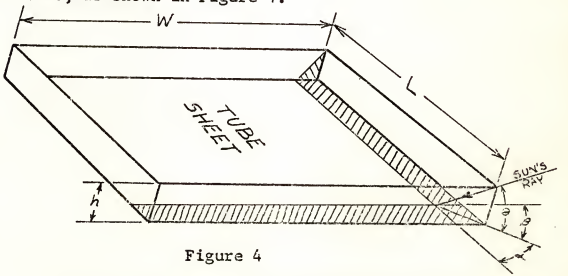

Figure 4

A well-designed solar collector-generator will have a glass surface area equal to the collector surface area,

so that at normal solar incidence, $S = 0$ in the $(1 - S)$ factor. However, this favorable angle of incidence can occur only at solar noon and only during a short period of the season, when the solar collector-generator is favorably inclined.

At all other times the tube sheet will be at least partially shaded. As is shown in Figure 4, the width W of sunlit tube sheet surface is reduced by the amount $h \cot \theta \cos \beta$. The length L is similarly reduced by the amount $h \cot \theta \cos \beta$. The parameter S is calculated thus:

$$S = \frac{Lh \cot \theta \cos \beta + Wh \cot \theta \cos \alpha - (h \cot \theta \cos \beta)(h \cot \theta \cos \alpha)}{WL}.$$

Obviously, to minimize this undesirable shading, the collector-generator should be designed as shallow as possible.

Now consider the effect of the tube and tube spacer (or backing sheet) geometry on the conduction of heat through the various configurations of the tube spacer and tube toward the refrigerant fluid in the tubes.

Transmission Through the Tube Sheet

For convenience, it is assumed that the tube sheet is in thermal contact with its surroundings only by way of the net radiant energy arriving at the upper surface,

with perfect insulation below.

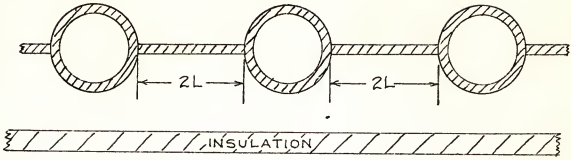

Figure 5

The net heat collected is the amount absorbed by the tube sheet minus the amount lost:

$$Q_{COLL} = \alpha I - (\epsilon h_r + h_a)(T_p - T_A) \quad . \qquad (1)$$

With no edge losses, and due to the symmetry of the tube and tube spacer pattern, the entire tube sheet of the collector-generator can be considered as a set of individual and identical, adjacent finned tubes, with zero heat losses at the fin extremities due to the temperature symmetry.

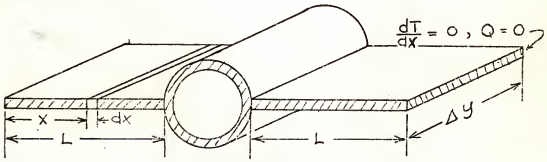

Figure 6

Assume that the above segment of a solar collector-generator tube and adjacent half spacers (fins) are being

uniformly irradiated from above and that one-dimensional heat flow is occurring along the fins from the extremities toward the tube which is at some constant temperature. Neglect any temperature variation along the tube axis and consider only a segment of width Δy measured in a direction parallel to the tube axis.

The conduction heat flow area is

$$A_F = B \Delta y .$$

At location X , the rate of heat collection is

$$Q_{u-x} = Q_A - U_L (T_p - T_A). \qquad (2)$$

The heat flow through the fin at this location is

$$Q = -K A_F \frac{dT_p}{dx} = -KB \Delta y \frac{dT_p}{dx}. \qquad (3)$$

The heat gain through the area $\Delta y dx$ on top of the fin element is

$$\frac{dQ}{dx} dx = -KB \Delta y \frac{d^2 T_p}{dx^2} dx. \qquad (4)$$

In terms of heat collected, this can be expressed as

$$\frac{dQ}{dx} dx = Q_{u-x} \Delta y \, dx. \qquad (5)$$

Combining equations 2, 4, and 5,

$$\frac{d^2T_P}{dx^2} = \frac{U_L}{KB}\left[\left(T_P - T_A\right) - \frac{Q_A}{U_L}\right].$$

This differential equation has the general solution:

$$T_P = C_1 e^{bx} + C_2 e^{-bx} + T_A + \frac{Q_A}{L}. \quad (6)$$

The constants C_1 and C_2 are determined by the boundary conditions:

$$\left.\frac{dT_P}{dx}\right)_{x=0} = 0 \qquad \text{and} \qquad \left.T_P\right)_{x=L} = T_T .$$

$$C_1 = C_2 = \frac{T_T - T_A - Q_A/L}{e^{bL} - e^{-bL}} . \quad (7)$$

With this substitution the equation becomes

$$T_P = T_T\left[\frac{\cosh bx}{\cosh bL}\right] + \left[T_A + \frac{Q_A}{Q_L}\right]\left[1 - \frac{\cosh bx}{\cosh bL}\right]. \quad (8)$$

Since the average heat collection rate is equal to the total heat flow at the tube junction divided by the surface area,

$$Q_{c,AVE.} = \frac{Q_{x=L}}{L\Delta y} .$$

From equation 3

$$Q_u = \frac{Q_{x=L}}{L\Delta y} = \frac{-KB}{L}\frac{dT_P}{dx} . \quad (9)$$

Differentiating equation 8 and substituting in equation 9 [19],

$$Q_c = \underbrace{\frac{\tanh bL}{bL}}_{\text{TUBE SHEET OR FIN EFFICIENCY}} \underbrace{\left[Q_A - U_L (T_T - T_A) \right]}_{\text{USEFUL COLLECTION RATE IF THE ENTIRE FIN WERE AT THE TEMPERATURE OF THE TUBE JUNCTION}} . \qquad (10)$$

In this investigation, an integral tube sheet configuration was not used in building the collector-generator because of the cost. Instead, a grid of pipes bonded to a backing sheet was made up from available material. In cross-section, the configuration is as shown in Figure 7.

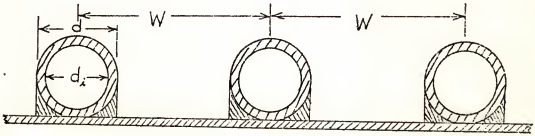

Figure 7

To analyze the heat transfer through this type of configuration, consider such an array of equally spaced parallel tubes with outside diameter d and inside diameter d_i, spaced W feet on centers and bonded to a single backing sheet or collector plate. The bond width will be assumed to be the same as the tube outside diameter.

The thermal conductivity of this bond will be designated as U_c BTU/HR-FT^2 .

The following simplifying assumptions will be made:

1. The tube wall resistance is negligible as compared to all other thermal resistances.

2. The division of sunshine reaching the plate is such that the fraction d/W is absorbed on the tubes and $(1 - d/W)$ is absorbed by the plate.

3. The loss rate factors of the tubes and of the backing sheet are proportional to the ratios of their projected areas d/W and $(1 - d/W)$ respectively.

The following heat transfer rates can be written, all on the per-square-foot-of-collector basis:

The useful heat gain from the sunshine striking the tubes is

$$Q_{u\text{-TUBES}} = \frac{d}{W}\left[Q_A - \epsilon R - U_L(T_T - T_A)\right]. \quad (11)$$

The useful heat gain from the sunshine striking the backing sheet is

$$Q_{u\text{-PLATE}} = \left(1 - \frac{d}{W}\right)F\left[Q_A - \epsilon R - U_L(T_T - T_A)\right]. \quad (12)$$

The heat transfer through the bond is

$$Q_{u\text{-PLATE}} = \frac{d}{W}U_c(T_c - T_T). \quad (13)$$

The heat transfer from the tube to the fluid is

$$Q_u = \frac{\pi d_i h_c}{W} (T_T - T_A) . \qquad (14)$$

The total useful heat gain is

$$Q_u = Q_{u-TUBES} + Q_{u-PLATE} . \qquad (15)$$

The simultaneous solution of the above set of five equations involves fifth order determinants. The rather voluminous computations have been carried out by Bliss [19] and the result is

$$F' = \frac{1}{\frac{W U_L}{\pi d_i h_c} + \frac{1}{\frac{d}{W} + \frac{1}{\frac{W U_L}{d U_c} + \frac{1}{1 - \frac{d}{W} F}}}} . \qquad (16)$$

where F' is the overall collection plate efficiency factor for the configuration with tubes bonded to a backing sheet and F is the fin efficiency factor as defined previously in equation 10 for the integral tube sheet collector configuration.

In the case where the resistance of the tube bond is negligible, $\frac{1}{U_c} = 0$, and equation 16 reduces to

$$F' = \frac{1}{\frac{W U_L}{\pi d_i h_c} + \frac{1}{\frac{d}{W} + \left(1 - \frac{d}{W}\right) F}} . \qquad (17)$$

Actual calculation of typical resistances of the tube walls and convective films shows that the assumption made above, that the tube wall resistance is negligible, is reasonable. Furthermore, this justifies the assumption that the entire tube circumference is at some constant temperature, at least where single-phase flow inside the collector-generator tube is concerned.

This single-phase flow will occur at the lower entrance regions of the collector-generator tubes where the subcooled strong ammonia liquor is fed to the inclined tubes of the tube sheet. At the low liquid flow rates anticipated, laminar, single-phase flow should occur at least up to the location where the mixture reaches the saturation temperature. This heat transfer to the single-phase fluid from the heated tubes will be treated in the following section.

Transmission to the Refrigerant Fluid in the Single-Phase Region

The basic equations for conservation of energy, conservation of momentum, and continuity will apply for the single-phase flow occurring in the collector-generator tubes. These expressions are commonly written in vector notation and for energy, momentum, and continuity are, respectively:

$$\frac{DT}{d\tau} = \alpha \nabla^2 T , \qquad (18)$$

$$\frac{D\vec{\omega}}{d\tau} = \bar{g} - \frac{1}{\rho} \text{ grad } P + \nu \nabla^2 \vec{\omega}, \text{ and} \qquad (19)$$

$$\frac{d\vec{\omega}}{d\tau} = 0 .$$

For laminar, steady flow in a tube, $\frac{D\vec{\omega}}{d\tau} = 0$, and where the laminar velocity profile is assumed independent of gravity effects, equation 19 becomes

$$-\frac{dP}{dx} + \mu\left(\frac{d^2\omega}{dR^2} + \frac{1}{R}\frac{d\omega}{dR}\right) = 0 , \text{ or}$$

$$\frac{d}{dR}\left(2\pi R \mu \frac{d\omega}{dR}\right) = 2\pi R \frac{dP}{dx} . \qquad (20)$$

Upon integration, this becomes

$$\mu \frac{d\omega}{dR} = \frac{R}{2}\frac{dP}{dx} + C_1 .$$

Since $\left.\frac{d\omega}{dR}\right)_{R=0} = 0$ due to symmetry, $C_1 = 0$.

Integrating again, and applying the boundary condition $\omega)_{R=R_i} = 0$, the velocity distribution becomes

$$\omega = -\frac{1}{4\mu}\frac{dP}{dx}\left(R_i^2 - R^2\right).$$

The average velocity is

$$\bar{\omega} = \frac{1}{\pi R_i^2} \int_0^{R_i} 2\pi R \omega \, dR = \frac{R_i^2}{8\mu} \frac{dP}{dX} .$$

Thus, in terms of average velocity $\bar{\omega}$, the general expression for the laminar velocity profile becomes

$$\omega = 2 \bar{\omega} \left[1 - \left(\frac{R}{R_i} \right)^2 \right] . \qquad (21)$$

The energy equation 18 for symmetrical flow is

$$K \left(\frac{\partial^2 T}{\partial R^2} + \frac{1}{R} \frac{\partial T}{\partial R} + \frac{\partial^2 T}{\partial R^2} \right) = c\rho \left(\frac{\partial T}{\partial \tau} + \omega_R \frac{\partial T}{\partial R} + \omega_x \frac{\partial T}{\partial X} \right) \qquad (22)$$

Again, for fully developed, steady, symmetric flow, $\frac{\partial T}{\partial \tau} = 0$, and combining equations 21 and 22,

$$\frac{\partial^2 T}{\partial R^2} + \frac{1}{R} \frac{\partial T}{\partial R} = \frac{2\bar{\omega}}{\alpha} \left[1 - \left(\frac{R}{R_i} \right)^2 \right] \frac{\partial T}{\partial X} - \frac{\partial^2 T}{\partial X^2} . \qquad (23)$$

This equation can be simplified by introducing the Peclet number, $Pe = \frac{\bar{\omega} D}{\alpha}$ and the following dimensionless coordinates [20] :

$$\Theta = \frac{T_w - T}{T_w - T_i} , \quad \epsilon = \frac{R}{R_i} , \quad \bar{X} = \frac{X}{R_i}$$

$$\frac{\partial^2 \Theta}{\partial \epsilon^2} + \frac{1}{\epsilon} \frac{\partial \Theta}{\partial \epsilon} = Pe (1 - \epsilon^2) \frac{\partial \Theta}{\partial \bar{X}} - \frac{\partial^2 \Theta}{\partial \bar{X}^2} . \qquad (24)$$

The last term, $\frac{\partial^2 \Theta}{\partial X^2}$, can be shown to be negligibly small in order of magnitude. The remaining equation can be partially solved by assuming a product solution of the form

$$\Theta = \psi(\epsilon)\, e^{-\frac{\beta^2 X}{Pe}} .$$

With this substitution, equation 24 becomes the following ordinary differential equation:

$$\frac{d^2\psi}{d\epsilon^2} + \frac{1}{\epsilon}\frac{d\psi}{d\epsilon} + \beta^2(1-\epsilon^2)\psi = 0 .$$

This is recognized as the modified Bessel's equation and, given the boundary conditions existing at the entrance section of the collector-generator tubes, it can be solved by the classical methods.

The preceding analysis will apply only to lower sections of the collector-generator tubes where the entering liquid refrigerant is subcooled. In the following analyses, the effects of vapor generation on the heat transfer to the two-phase mixture in the collector-generator tubes will be considered.

Bubble Growth and Motion in the Collector-Generator Tubes

The physical condition of the inner surfaces of the collector tubes will have an important bearing on the

initiation of vapor bubbles when the tube walls become heated, since it has been shown that surface roughness, microcavities, foreign particles, and other irregularities can serve as nucleation sites for the vapor bubbles. Without these nucleation sites, vapor bubbles theoretically could not start to form without degrees of superheat far in excess of those experimentally observed.

Now consider a spherical bubble starting to form at some microcavity or irregularity on the inner surface of a collector-generator tube and at equilibrium with its surrounding fluid. To find an expression for the degrees of superheat required to initiate the bubble formation, the force equation (to be derived later) is written first:

$$P_V - P_L = \frac{2\sigma}{R} . \qquad (25)$$

With a perfect gas, the Clausius-Clapeyron equation is, along the saturation line,

$$\frac{dP}{dT} \cong \frac{h_{fg} P_V}{T_V} \cong \frac{h_{fg} P_V}{R_V T_V^2} . \qquad (26)$$

$$\text{also,} \quad P_V - P_L \cong \left(T_V - T_{SAT}\right) \frac{dP}{dT} . \qquad (27)$$

Integrating equation 26 and combining with 25 and 27, the following expression is obtained:

$$T_v - T_{SAT} = \frac{R_v T_{SAT} T_v}{h_{fg}} \ln\left(1 + \frac{2\sigma}{P_L R}\right). \qquad (28)$$

Since $(T_v - T_{SAT})$ is very small for high pressures, such as those which will exist in the collector-generator, equation 28 then simplifies to

$$T_v - T_{SAT} \cong \frac{2 R_v T_{SAT}^2 \sigma}{h_{fg} P_L R}. \qquad (29)$$

This is approximately the superheat required for a bubble of radius R, and, theoretically, bubbles of a smaller radius will collapse and bubbles of a larger radius will grow.

The first consideration, once the bubble has started to grow on the surface of the collector-generator tube, is the rate of heat transfer to the bubble. To analyze this, consider first a system comprising a spherical bubble.

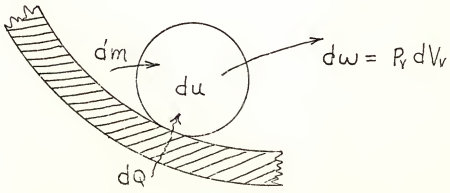

Figure 8

The energy equation is:

$$dQ = dm\, h_{fg} + du + P_v\, dV_v . \qquad (30)$$

Since the pressure of the vapor within the bubble is greater than that of the surrounding fluid because of the surface tension at the curved interface, the force equation for the stationary bubble system is:

$$\Sigma F_y = (P_v)_y - (P_L)_y - 2\pi R\sigma = 0$$

and $\pi R^2 (P_v - P_L) = 2\pi R\sigma$,

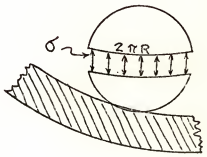

Figure 9

giving equation 25:

$$P_v - P_L = \frac{2\sigma}{R} .$$

Thus the energy equation becomes

$$dQ = dm\, h_{fg} + du + \left(\frac{2\sigma}{R} + P_L\right) dV_v , \text{ OR}$$

$$dQ = h_{fg}\, d(V_v \rho_v) + \left(\frac{2\sigma}{R} + P_L\right) dV_v + du . \qquad (31)$$

For a spherical bubble with no internal energy change $V = \frac{4}{3}\pi R^3$ and $dV = 4\pi R^2$. Thus, with ρ_v constant,

$$dQ = 4\pi R^2 \left(h_{fg}\rho_v + \frac{2\sigma}{R} + P_L\right).$$

Integrating from R=0 (bubble initiation) to R= R

$$Q = \frac{4}{3}\pi R^3 \left(h_{fg}\rho_v + \frac{2\sigma}{R} + P_L\right).$$

The three terms on the right represent, respectively, the vaporization energy, the work of expanding the surface tension "film," and the work of pushing back the surrounding fluid [21].

Determining the rate of bubble growth while attached to the heated tube wall is somewhat more complex and involves the solution of a partial differential equation derived by Rayliegh in 1917 [22]:

$$R\frac{\partial^2 R}{\partial T^2} + \frac{3}{2}\left(\frac{\partial R}{\partial T}\right)^2 + \frac{2\sigma}{\rho_L R} = \frac{P_v - P_L}{\rho_L}. \qquad (32)$$

Fritz and Ende [23] formulated a solution of Rayliegh's equation of the following form which has been shown to approximate the experimental data [24]:

$$R = \frac{2(T_w - T_{SAT})\, C_p \rho_L}{\rho_v h_{fg}} \sqrt{\frac{\alpha t}{\pi}}. \qquad (33)$$

Once the bubble has reached a size where buoyant forces of the surrounding fluid in the collector-generator tube become significant, it will grow only until it reaches a characteristic departure diameter determined by the dynamics of the surrounding refrigerant fluid, as well as by the buoyant and adhesive forces at the collector-generator tube surface. A complete analysis of the bubble system at departure is not available in the literature but Fritz [25], considering only the buoyant and adhesive forces, proposed the following expression for the bubble radius at departure:

$$R_D = 0.021\ \theta \sqrt{\frac{\sigma}{g(\rho_L - \rho_v)}} \quad . \tag{34}$$

where θ is the contact angle in degrees.

Once the bubble has left the heated collector-generator tube surface it will start to rise in the surrounding fluid until it strikes the upper tube wall, then follow this wall in an axial direction and eventually reach the liquid surface.

If the surrounding refrigerant fluid is at saturation temperature, the heat effects will be of lesser importance than the dynamic forces in determining the rise velocity of the bubble [21].

Now, consider a bubble that has reached the departure radius and has just left a spot on the collector-generator tube surface, and has started to rise into the surrounding fluid.

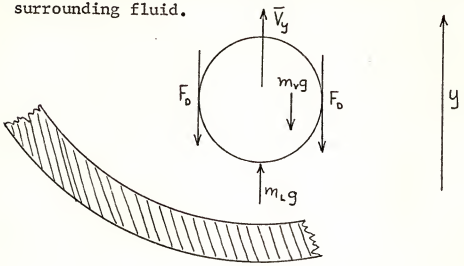

Figure 10

For the isolated bubble system shown, the momentum equation is

$$\Sigma F_y = \frac{d}{dt}(m_v \bar{V}_y) = (m_L g - m_v g)\frac{1}{g_c} - F_D, \text{ or}$$

$$m_v \frac{d\bar{V}_y}{dt} + \bar{V}_y \frac{dm_v}{dt} = (m_L - m_v)\frac{g}{g_c} - F_D \ . \qquad (35)$$

Since it has been observed that a rising bubble quickly reaches a terminal velocity, the acceleration term on the left side of the equation will be neglected. Also, if there is no further condensation or vaporization into or out of the bubble system, the bubble will be assumed to have constant mass, and $\frac{dm_v}{dt} = 0$. (This will be

approximately the case existing in the nucleate boiling regions of the collector-generator tubes, since it is assumed that the surrounding refrigerant fluid is saturated.) Thus, equation 35 is reduced to the following expression for the drag force acting on a bubble during the time it is rising vertically in the refrigerant fluid in a collector-generator tube:

$$F_D = (m_L - m_V)\frac{g}{g_c} = \frac{4}{3}\pi R^3(\rho_L - \rho_V)\frac{g}{g_c} . \qquad (36)$$

It can be seen that the drag force on the bubble acts similarly to that resisting force acting on a sphere moving steadily through a viscous fluid. Thus, the problem of the bubble rising in the collector-generator tubes can be thought of as a problem in hydrodynamics. This particular problem was solved by Stokes in 1854 [26] . His solution for the drag force acting on a sphere of radius R was:

$$F_D = \frac{6\pi R \mu \bar{V}}{g_c} . \qquad (37)$$

To obtain an expression for the rise velocity of a bubble in the collector-generator tube, equations 36 and 37 are solved for F_D and the following result is obtained:

$$\bar{V} = \frac{2R^2(\rho_L - \rho_V)}{9\mu} . \qquad (38)$$

This result agrees very closely with experimental observations [27] of bubble rise velocities where the bubble Reynolds number, Re_B, is less than 2. Re_B is defined as

$$Re_B = \frac{2R\bar{V}\rho_L}{\mu_L}.$$

The drag coefficient for bubbles with $Re_B \leq 2$ is

$$C_D = \frac{24}{Re_B} \quad , \text{ where } \quad C_D = \frac{2g_c F_D}{\rho_L \bar{V}_B^2 A}.$$

For bubble sizes in the range $2 \leq Re_B \leq 200$, Robinson [28] found $C_D = 18.5/(Re_B)^{0.6}$.

For convenience, up to this point in the analysis, only the individual bubbles have been considered. However, the bulk flow of vapor along the collector-generator tube walls will have important effects on the heat transfer to the fluid from the heated tube walls. This bulk flow of vapor will be made up of the many bubbles of vapor boiled out of the refrigerant fluid in the collector-generator tubes.

As an introduction to the rather restricted boiling pattern which occurs within an inclined collector-generator

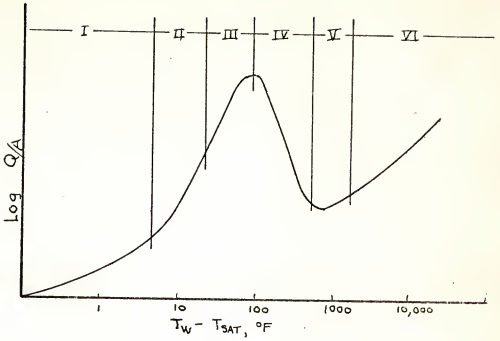

Figure 11[29]

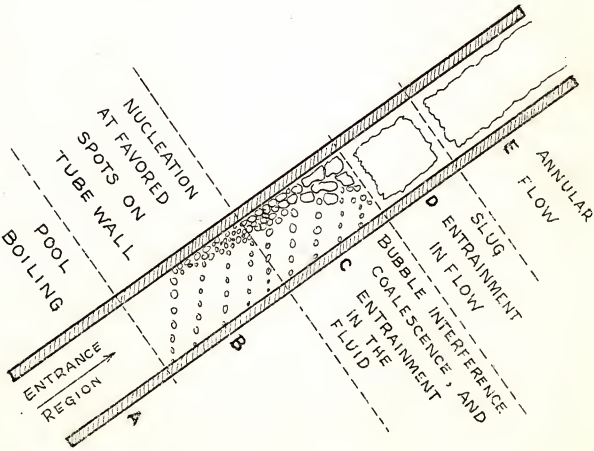

Figure 12 [31]

tube, consider first the several types of boiling which can occur at a heated surface in a "free" liquid, and then compare these phenomena to the types of boiling that have been observed inside vertical and inclined tubes.

Figure 11 illustrates the regimes of boiling heat transfer in a free liquid [29].

The boiling regimes shown in Figure 11 have a correspondence with the types of two-phase flow that can occur with various heat transfer rates in an inclined tube such as that in a collector-generator. To show this correspondence compare the regimes of Figure 11 to the various flow regimes that have been observed in vertical or inclined tubes as shown in Figure 12.

Region A in Figure 12, which represents the single phase flow at the entrance of a collector-generator tube, corresponds to Regime I of Figure 11. Regions B and C correspond to Regime II and part of Regime III. At the higher heat transfer rates of Regime III and for at least part of Regime IV, Region D would correspond, with transition from slug flow to annular flow probably occurring without a distinct transition point, since this is a very unstable type boiling.

In the collector-generator tubes, Regions A, B, and C, and Regimes I, II and III will represent the usual types of flow and heat transfer occurring, although it is possible that Region D or E type flow could occur.

If a sudden, heavy refrigeration load is applied by opening the expansion valve too quickly, the resulting high rate of vapor evolution along the inclined tubes could cause slugging or boil-over into the condenser.

In the regime of nucleate boiling which will occur along the collector-generator tubes, there will be a bulk flow of vapor along the upper segment of the tube flow section, as shown in Figure 13.

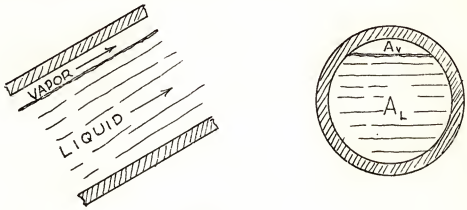

Figure 13

This segment of vapor, consisting of the accumulation of vapor bubbles rising along the collector-generator tubes, will affect the heat transfer from the heated tube walls to the refrigerant fluid, depending on the magnitude of the vapor fraction, which is defined as the ratio

$$\frac{\text{FLOW AREA OF THE VAPOR}}{\text{TOTAL CIRCULAR FLOW AREA}} = \frac{A_V}{A_T} .$$

Although preliminary calculations show that the vapor fractions occurring in the collector-generator tubes will be less than 5 per cent, the general problem of the effect of the vapor flow upon the heat transfer to the refrigerant fluid in an inclined tube will be considered in the following section.

The Effects of the Vapor Fraction on Two-Phase Heat Transfer in the Inclined Collector-Generator Tubes

For this analysis, select an elemental section of a heated tube of inside diameter D inclined at an angle ϕ above the horizontal.

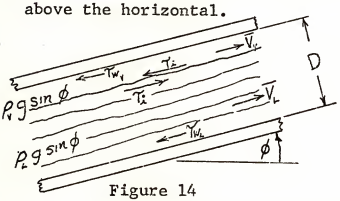

Figure 14

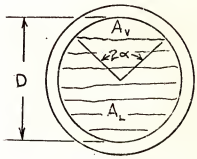

Figure 15

Momentum equation for the vapor:

$$\frac{dP}{dx} A_v - \tau_i D \sin\alpha - \tau_{w_v} \alpha D =$$

$$\frac{d}{dx}(m_v \bar{V}_v)\frac{g}{g_c} - \bar{V}_L \frac{dm_v}{dx}\frac{g}{g_c} - \rho_v A_v g \sin\phi \, dx. \qquad (39)$$

Momentum equation for the liquid:

$$-\frac{dp}{dx}A_L - \tau_i D \sin\alpha - \tau_{w_L}(\pi-\alpha)D = \frac{d}{dx}(m_L\bar{V}_L)\frac{g}{g_c} + \bar{V}_L\frac{dm_v}{dx}\frac{g}{g_c} - \rho_L A_L g \sin\phi\, dx \,. \quad (40)$$

Energy equations:

$$\frac{\bar{q}}{A}\pi D dx = m_v h_{fg} \,, \text{ or } \frac{dm_v}{dx} = \frac{\bar{q}}{A}\frac{\pi D}{h_{fg}} \,. \quad (41, 42)$$

Continuity equations:

$$m_v = \rho_v A_v \bar{V}_v \quad , \quad m_L = \rho_L A_L \bar{V}_L \,. \quad (43)$$

To arrive at an expression for the vapor fraction A_v/A_T, the reasonable assumption is made that, within the elemental section dx, the pressure drop across the vapor is of the same value as the pressure drop across the liquid. Then, in equations 39 and 40, $\frac{dp}{dx}$ is eliminated with the following result:

$$\frac{1}{A_v}\left[-\tau_i D \sin\alpha - \tau_{w_v}\alpha D - \frac{d}{dx}(m_v\bar{V}_v)\frac{g}{g_c} + V_L\frac{dm_v}{dx}\frac{g}{g_c} + \rho_v A_v g \sin\phi\, dx\right] =$$

$$\frac{1}{A_L}\left[\tau_i D \sin\alpha - \tau_{w_L}(\pi-\alpha)D - \frac{d}{dx}(m_L\bar{V}_L)\frac{g}{g_c} - V_L\frac{dm_v}{dx}\frac{g}{g_c} + \rho_L A_L g \sin\phi\, dx\right] . \quad (44)$$

This can be reduced to a useful form if certain simplifications are made. An order of magnitude analysis of the friction forces acting and of the gravity effects on the area ratios indicates that the shear terms and the gravity terms may be neglected insofar as their effects on the changes in area ratios are concerned. For flow configurations such as a tube in a solar collector-generator, where the mass flow of the vapor is small as compared to the total mass flow rate, the terms controlling the vapor fraction are those for the momentum changes in the vapor caused by the addition of vapor to the vapor flow by evaporation occurring in the elemental length [30]. If we equate these significant terms, eliminating the velocity variables by means of the continuity equations, the following expression is obtained:

$$\frac{dA_L}{dx} = -2\,\frac{m_v}{m_L^2}\,\frac{\rho_L}{\rho_v}\,\frac{A_L^3}{A_v^2}\,\frac{dm_v}{dx}. \qquad (45)$$

Using the energy equations 41 and 42 to eliminate m_v and $\frac{dm_v}{dx}$, equation 45 becomes

$$\frac{dA_L}{dx} = -\frac{2}{m_L^2}\,K\,x\,\frac{\rho_L}{\rho_v}\,\frac{A_L^3}{A_v^2}, \quad \text{or}$$

$$\frac{dA_L}{dx} = \frac{-2K^2}{m_L^2}\frac{\rho_L}{\rho_V}\frac{A_L^3}{(A_T - A_L)^2} , \qquad (46)$$

where $K \equiv \frac{\bar{q}}{A}\frac{\pi D}{h_{fg}}$, and $A_T \equiv A_V + A_L$.

Separating the variables in equation 46 and integrating, the following expressions are obtained.

$$\frac{A_T^2 - 2A_T A_L + A_L^2}{A_L^3} dA_L = \frac{-2K^2}{m_L^2}\frac{\rho_L}{\rho_V} x\,dx .$$

$$-\frac{1}{2}\frac{A_T^2}{A_L^2} + 2\frac{A_T}{A_L} + \ln A_L = -\frac{2K^2}{m_L^2}\frac{\rho_L}{\rho_V}\frac{x^2}{2} - C .$$

$$\left(\frac{A_T}{A_L}\right)^2 - 4\frac{A_T}{A_L} - 2\ln A_L = \frac{2K^2\rho_L}{m_L^2\rho_V} x^2 + C .$$

Applying the boundary condition $A_L\big)_{x=0} = A_T$, i.e. vaporization begins at $X = 0$, the value of the constant C is:

$$C = -3 - 2\ln A_T .$$

Finally the equation becomes:

$$\left(\frac{A_T}{A_L}\right)^2 - 4\left(\frac{A_T}{A_L}\right) + 2\ln\frac{A_T}{A_L} + 3 = 2\left[\frac{\bar{q}}{A}\frac{\pi D}{h_{fg}}\right]\frac{X^2}{m_L^2}\frac{\rho_l}{\rho_v} . \qquad (47)$$

From the geometry of circular areas and segments expressed in polar coordinates, as shown in Figure 15, the liquid fraction is:

$$\frac{A_L}{A_T} = \left[1 - \left(\frac{\alpha}{\pi} - \frac{1}{2\pi}\sin 2\alpha\right)\right],$$

and the vapor fraction is:

$$\frac{A_v}{A_T} = \left[\frac{\alpha}{\pi} - \frac{1}{2\pi}\sin 2\alpha\right]. \qquad (48)$$

Obviously, since the desired expression $\frac{A_v}{A_T}$ is not explicit in equation 47, an iterative solution will be needed to evaluate the vapor fraction as a function of tube length X . If, as was assumed for the collector-generator tubes, the calculated vapor fraction proves to be small, the assumption of a mean heat transfer rate $\frac{\bar{q}}{A}$ in equations 41 and 42 is reasonable and could be closely approximated by $\frac{\bar{q}}{A'_L}$, where A'_L is the collector-generator tube surface area wet by the liquid refrigerant.

Thus, in the solar collector-generator tubes, the distribution of convective heat transfer area between that

of the ammonia liquor film and that of the ammonia vapor film will be determined by equations 47 and 48. Fortunately, under the usual, steady operating conditions, the vapor fraction will remain small in the collector-generator tubes. Thus, almost all the tube walls will be wet by the refrigerant fluid, giving better heat transfer than would result if a large proportion of the tube walls were in contact with the vapor.

The energy flow starting as incident solar energy has been traced through the many complex paths of the entire collector-generator unit. Now that it has finally emerged as the latent heat of vaporization of ammonia, the next consideration will be to relate this ammonia generating function of the solar collector-generator to that of the other components making up the complete absorption refrigeration system.

The Theory of Operation of the Complete Solar Driven Refrigeration System

The ammonia generating function of the collector-generator and the part it plays in the complete system can be made clear by following, in the diagram below, the flow of energy and fluids through the various components of the system. Since there is a distinct separation of dry ammonia vapor flow and the flow of the ammonia water solution, the system is best described by considering each of these

sections in turn.

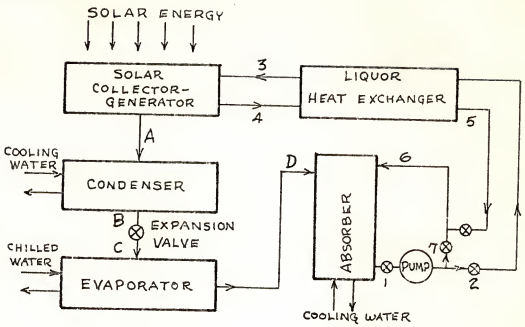

Figure 16

Ammonia Section

The left half of the flow diagram represents the actual cooling part of the system. Starting with the collector-generator, it can be seen that its function is to convert solar energy input to ammonia vapor output. The ammonia vapor given off by the collector-generator at A is led to a water cooled condenser. Here, the vapor gives up heat and becomes liquid ammonia.

This high pressure liquid is allowed to expand from B to C to a lower pressure in the evaporator. Further evaporation of the liquid ammonia occurs here and the resulting absorption of heat is used to chill water for refrigeration or air-conditioning. The ammonia vapor

leaves the evaporator and enters the absorber at D where it is drawn by its high affinity for water. Coming in contact with the spray mist in the absorber, the ammonia vapor is dissolved in the water, the heat of solution being carried away by the absorber cooling water.

Ammonia Liquor Section

This part of the system occupies the right half of the flow diagram. A strong ammonia-water solution of about 60 per cent ammonia by weight is pumped from the absorber at 1 through valve 2. Between 2 and 3 this cool liquor picks up some heat from the weak, hot liquor leaving the collector-generator at 4. At 3, the strong liquor enters the solar collector-generator wherein the solar heat boils off part of the ammonia. The resulting weaker liquor, of about 40 per cent concentration, is drawn off from the collector-generator at 4. Part of its heat is given up in the heat exchanger between 4 and 5. This weak solution is led into the absorber at 6 where it is sprayed as a fine mist to allow a large surface area of contact with the dry ammonia vapor entering the absorber at D. By recirculation of liquid around the flow loop 1, 7, 6, the ammonia liquor in the absorber can reach a concentration of about 60 per cent, depending on the cooling water temperature. The resulting strong liquor is then cycled again through the loop 1, 2, 3, 4, 5, 6. It should

be noted that this ammonia liquor loop performs the function of the compressor in a conventional ammonia compression refrigeration system, with the advantage that the absorption system requires a much smaller work input to the liquor pump.

To obtain a performance factor for the entire cycle, a heat balance is written for the refrigeration system. The First Law of Thermodynamics requires that the total energy added to the system from the surroundings must equal the energy rejected to the surroundings. If the pump work is neglected,

$$Q_{GEN} + Q_{EVAP} = Q_{ABS} + Q_{COND} . \qquad (49)$$

The performance factor is defined as follows:

$$P.F. = \frac{\text{REFRIGERATION EFFECT}}{\text{HEAT ADDED}} = \frac{Q_{EVAP}}{Q_{GEN}} . \qquad (50)$$

During steady state operation of the ideal closed cycle, the net entropy change of the fluid is ≥ 0 , i.e.,

$$\Delta S = \Delta S_{GEN} + \Delta S_{EVAP} + \Delta S_{o} \geq 0 .$$

$$\Delta S = -\frac{Q_{GEN}}{T_{GEN}} - \frac{Q_{EVAP}}{T_{EVAP}} + \frac{Q_{o}}{T_{o}} \geq 0 . \qquad (51)$$

Combining equations 49 and 51, the result is

$$Q_{GEN}\left(\frac{T_{GEN}-T_o}{T_{GEN}}\right) \geqslant Q_{EVAP}\left(\frac{T_o-T_{EVAP}}{T_{EVAP}}\right). \quad (52)$$

Now, equation 50 can be written:

$$P.F. = \frac{Q_{EVAP}}{Q_{GEN}} \geqslant \frac{T_{EVAP}\left(T_{GEN}-T_o\right)}{T_{GEN}\left(T_o-T_{EVAP}\right)}, \quad (53)$$

or, for a completely reversible system

$$P.F.\Big)_{MAX} = \frac{T_{EVAP}\left(T_{GEN}-T_o\right)}{T_{GEN}\left(T_o-T_{EVAP}\right)}. \quad (54)$$

It is interesting to note that equation 54 tells us that the maximum attainable performance factor for the absorption system is equal to the coefficient of performance for a Carnot refrigerating cycle working between temperatures T_{EVAP} and T_o multiplied by the efficiency of a Carnot engine working between the temperatures T_{GEN} and T_o. The equation also shows that the performance factor will increase with increase of the generator temperature T_{GEN} and with increase of temperature of the refrigerated region T_{EVAP}. The actual performance factor is usually much lower than that given by equation 54.

CHAPTER V

DESIGN OF THE MODEL

General Objectives

Among the factors important in the design of an operating solar collector-generator are, heat transfer characteristics, economics, fluid flow, corrosion resistance, and strength of materials. Taking these factors into account, the specific objectives in this design were:

1. To achieve the best heat transfer efficiency per unit cost of the collector-generator.
2. Allow for optimum vapor-liquid flow where these two phases appear together in the system.
3. To provide for complete separation of the vapor phase and the liquid phase at strategic points in the system.
4. To employ materials of construction that will resist corrosion by the highly alkaline ammonia solution.
5. To design all parts to withstand internal working pressures up to 200 pounds per square inch.

The latter two objectives were met by using standard steel pipe for all construction.

To meet the first objective, an analysis was made of the effects of several of the most important variables involved in the selection and placement of the pipes and

steel sheet used in making the collector-generator.

Design of the Tube Sheet

A frontal area of 4 by 4 feet having been chosen arbitrarily, the tube lengths were fixed at 48 inches. This left the following variables to be considered in meeting the first objective:

1. Center to center tube spacing - 2 to 10 inches.
2. Tube diameter - 3/4, 1, 1-1/4, and 1-1/2 inch O.D.
3. Sheet thickness - 1/16, 1/8, and 3/16 inch.

Using the efficiencies given in equations 10 and 17, calculations were made of the collector efficiency, and collector efficiency per unit weight. A series of calculations were made for each of the increments shown above. The results of these calculations are shown in Figures 17, 18, 19, and 20.

In addition to the effects just considered, the effects of tube diameter on the two-phase flow up the inclined tubes of the collector-generator were also considered.

In certain small tube sizes, it is possible that the bubble generation rate could be so high that the tube would be completely choked with vapor, greatly limiting the heat transfer to the liquid. To estimate a steady state maximum bubble formation rate, the total vapor

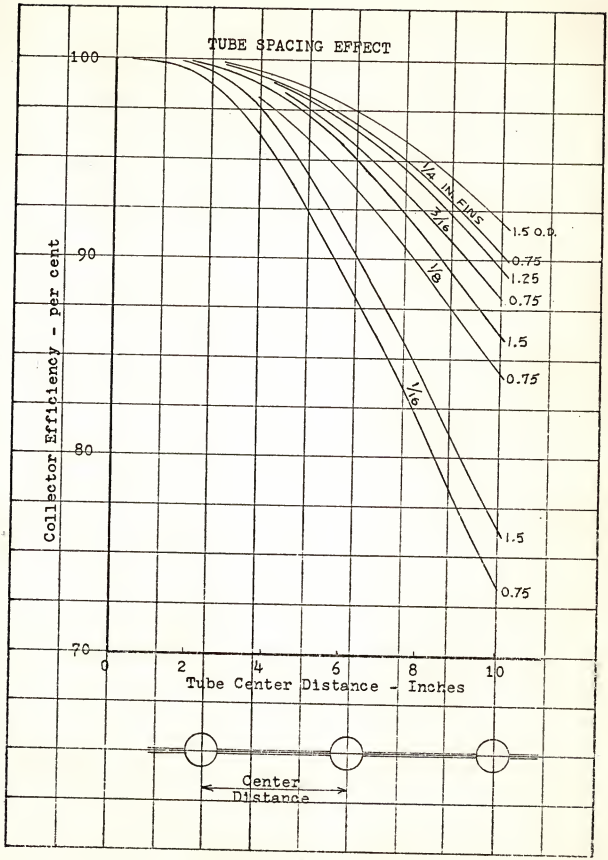
TUBE SPACING EFFECT
100
90
80
70
Collector Efficiency - per cent
0
2
4
6
8
10
Tube Center Distance - Inches
1/4 IN. FINS
3/16
1/8
1/16
1.5 O.D.
0.75
1.25
0.75
1.5
0.75
1.5
0.75
Center Distance

Figure 17

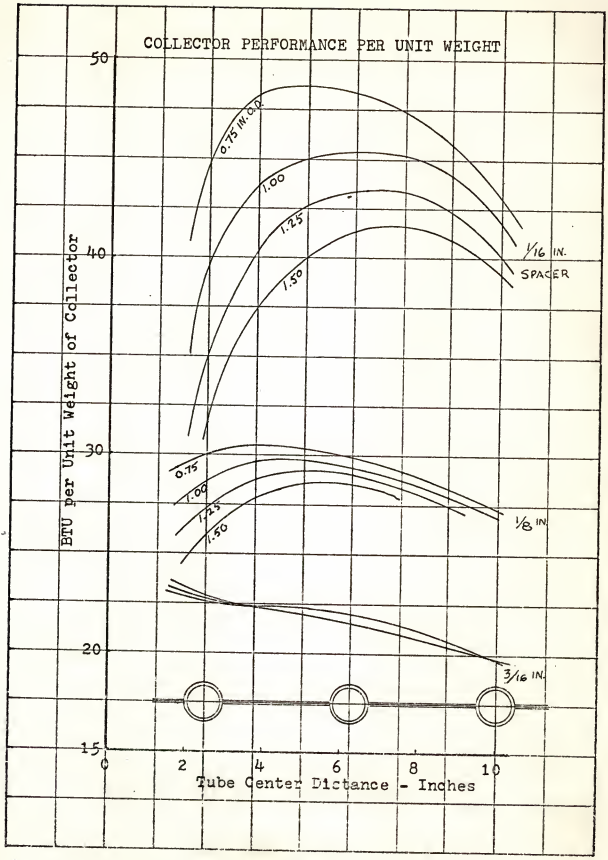
COLLECTOR PERFORMANCE PER UNIT WEIGHT
BTU per Unit Weight of Collector
50
40
30
20
15
0
2
4
6
8
10
Tube Center Distance - Inches
0.75 IN. O.D.
1.00
1.25
1.50
1/16 IN. SPACER
0.75
1.00
1.25
1.50
1/8 IN.
3/16 IN.

Figure 18

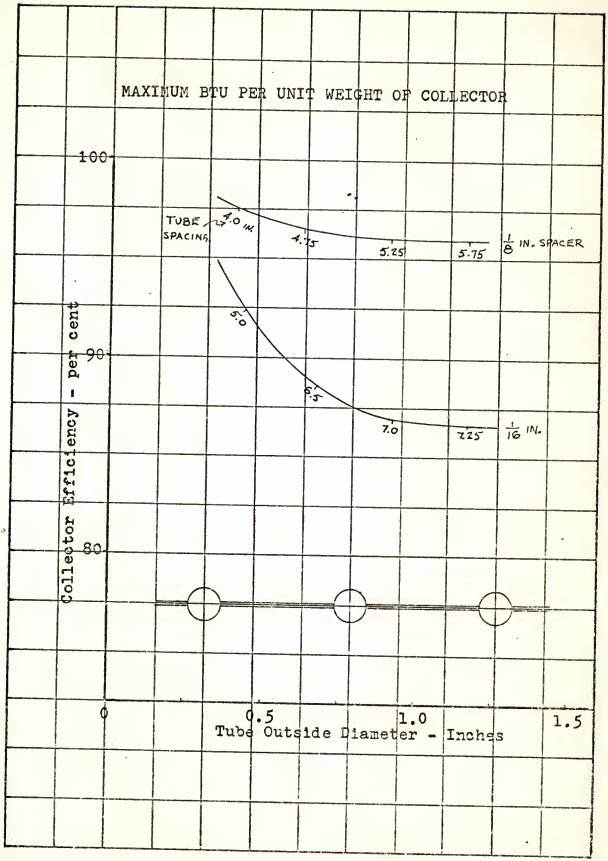
MAXIMUM BTU PER UNIT WEIGHT OF COLLECTOR
100
90
80
0
Collector Efficiency - per cent
TUBE SPACING
4.0 IN.
4.75
5.25
5.75
1/8 IN. SPACER
5.0
5.5
7.0
7.25
1/16 IN.
0.5
1.0
1.5
Tube Outside Diameter - Inches

Figure 19

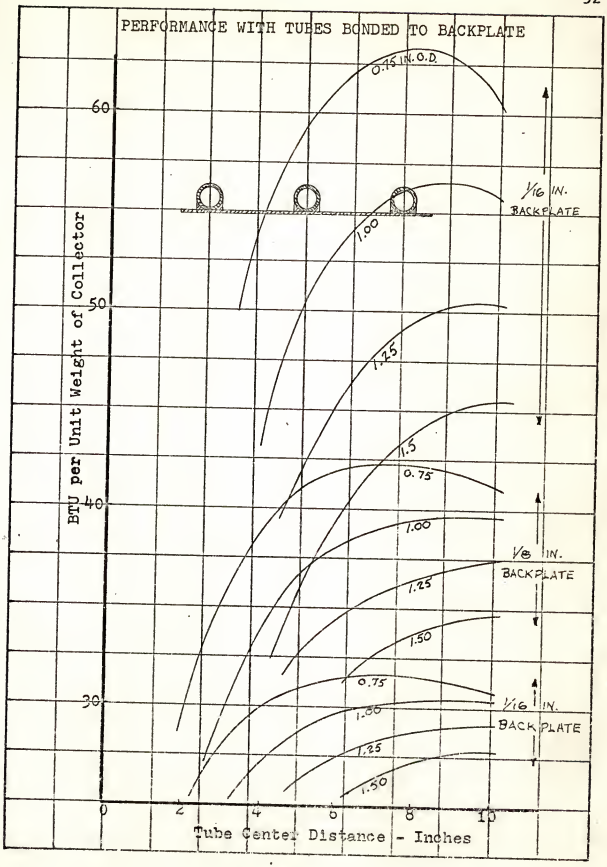
PERFORMANCE WITH TUBES BONDED TO BACKPLATE
BTU per Unit Weight of Collector
60
50
40
30
0
2
4
6
8
10
Tube Center Distance - Inches
0.75 IN. O.D.
1/16 IN. BACKPLATE
1.00
1.25
1.5
0.75
1.00
3/8 IN. BACKPLATE
1.25
1.50
0.75
1/16 IN. BACKPLATE
1.00
1.25
1.50

Figure 20

generation rate was calculated for the maximum possible heat transfer per tube. It was found that, for 1-inch diameter tubes spaced 4 inches on center, at the maximum possible insolation rate, a minimum average bubble rise velocity of 0.159 inches per second would be required to prevent any net accumulation of vapor in the immediate area where formed.

Jakob [33] measured vertical rise velocities of 13 inches per second for steam bubbles. If the order of magnitude of this measured velocity is representative for the collector-generator tubes, then no appreciable vapor accumulation should occur in 1-inch diameter tubes. However, the collector-generator tubes are not vertical.

Thus, further information was needed concerning the ratios of bubble flow velocities in inclined tubes to the velocities in vertical tubes. A search of the literature was made without success.

To expedite the design, a series of simple experiments were performed measuring the rise velocities of bubbles in an inclined tube. These experiments and their results are described in the next section.

The Effect of Tube Inclination on Two-Phase Flow

To approximate as closely as possible the diameter and length of the actual tubes in the collector-generator, the bubble flow experiment was devised using a glass tube

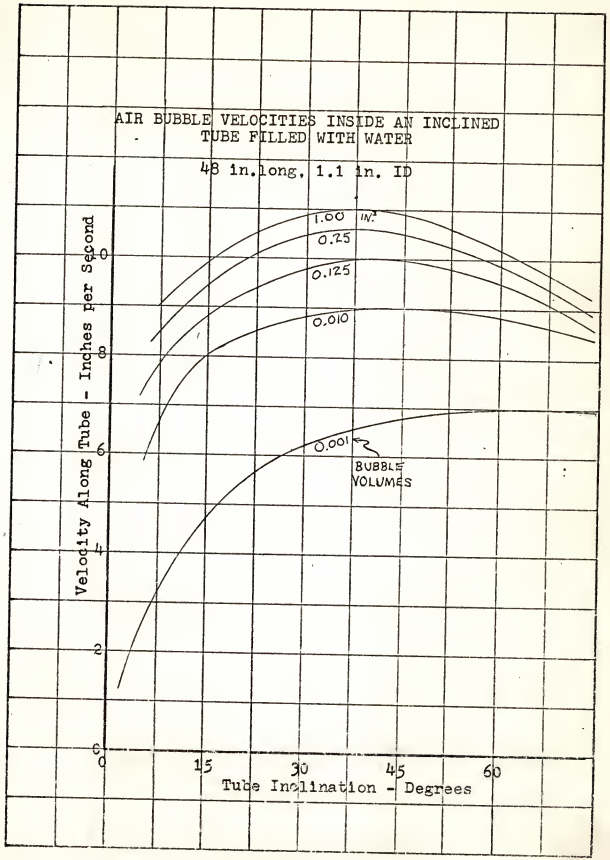
AIR BUBBLE VELOCITIES INSIDE AN INCLINED TUBE FILLED WITH WATER
48 in. long, 1.1 in. ID
Velocity Along Tube - Inches per Second
Tube Inclination - Degrees
0
2
4
6
8
10
15
30
45
60
1.00 IN.³
0.25
0.125
0.010
0.001
BUBBLE VOLUMES

Figure 21

48 inches long, and of 1.12 inches inside diameter. This tube was filled with water and arranged so that the rise time of air bubbles could be timed as the tube was inclined at each different angle.

The results of this series of experiments were quite significant and are shown in Figure 21. From the characteristic shown by the curves, and from other observations made during the experiments, the following useful conclusions can be made:

1. All the various sizes of bubbles quickly reached their terminal velocity for each of the different inclinations.

2. There was a very rapid increase of all bubble velocities as the inclination was increased from 1 degree to 5 or 10 degrees, with relatively little increase occurring in the range of inclinations from 15 to 75 degrees.

3. Most of the bubbles had a maximum velocity at inclinations between 30 and 45 degrees.

4. All the bubbles showed a decrease in net vertical velocity as the tube's inclination approached 90 degrees, due to the appearance of rapid, sidewise oscillations as the bubbles were freed from the tube wall guidance.

It is realized that air bubbles in water are different from ammonia vapor bubbles in an ammonia water solution. However, as was shown in Chapter IV, the hydrodynamics of bubbles are functions mainly of diameters, densities, and viscosities. If these parameters are similar, then the velocity effects will be similar. Thus, the vapor in the inclined collector-generator tubes

should rise as fast or faster than it would in vertical tubes. If this is true, then there should be no vapor choking in 1-inch diameter tubes due to vapor accumulation.

In addition to the two-phase flow effects considered above, the proper inclination of the collector tubes is influenced by another important factor. This is the variation of the solar incidence angle with the seasons and by the hour, which will be considered in the next section.

Effects of Changes in the Solar Incidence Angle

For the most favorable interception of solar energy, the collector-generator should be oriented and inclined so that the sun's rays are perpendicular to the plane of the collector at solar noon.

However, due to the thermal lag of the earth and its atmosphere, maximum air temperatures appear a month or more after summer solstice. Also, daily peaks in the cooling load usually occur 2 or 3 hours after noon, when the altitude angle of the sun will have decreased even more. For these reasons, selection of an angle of inclination somewhat higher than the best inclination at summer solstice is justified.

Other factors affecting the inclination and orientation of the solar collector-generator are: the latitude of the location, the hours of maximum use, pre-

vailing weather patterns, the nature of the surrounding objects, and many other minor considerations.

Summary of the Design Considerations and Choices

Tube Spacing

The curves of BTU per unit weight and of collection efficiency indicate that, within limits, tube spacing is not critical, and that it will be a compromise between efficiency and economy. A spacing of 4 inches on centers was chosen.

Tube Diameter

Figures 19 and 20 indicate that, although there is a slight increase in collection efficiency as the diameter is increased, no gain is achieved by any increase of tube diameter beyond 1 inch. Therefore, 1-inch standard steel pipe was selected for the 13 riser tubes in the collector-generator. This size also met the second general objective stated above.

Backing Sheet Thickness

The most efficient tube and sheet combinations call for sheet thickness far too heavy and costly. However, if efficiencies of about 75 per cent are acceptable, sheet thicknesses of 1/16 inch or less can be used, especially if there is a good thermal bond between the tube and the sheet.

A 20 gage steel sheet was soldered to the back of the collector tubes, with care being taken that the solder bonded to about 90^{o} of the pipe circumference.

Header for the Collector Tubes

To meet the third general objective, a large diameter header was made of a 52-inch length of 2-1/2-inch standard pipe. Thus when the collector-generator is filled to the half-way point in the header, a liquid surface of 130 square inches is provided to allow the emerging vapor bubbles to separate from the liquid with a minimum of liquid carryover into the condenser.

Inclination of the Collector-Generator

The bubble flow experiments, the two-phase flow consideration, and the solar incidence angle all point to a choice of inclination angle between 5 and 40 degrees. It was decided to sacrifice the better solar input at low angles of inclination for better flow characteristics at an angle of 30 degrees above the horizontal.

CHAPTER VI

AUXILIARY EQUIPMENT

General Procedure

This particular series of steps in the investigation was only indirectly concerned with the stated object of the thesis. Thus, since the optimum design of each refrigeration component is a complex problem in itself, after careful analysis of the theoretical requirements for the various components, commercially available parts were selected wherever possible. With the exception of valves and pipe fittings, all the basic components were machined and welded together by the writer from standard stock and parts.

Each component of the auxiliary system was essentially a special purpose heat exchanger. The condenser, absorber, and evaporator were of the shell and tube type. The liquor heat exchanger was made of two concentric pipes.

In estimating the areas of heat transfer surface needed for each unit, existing methods and commercially proven data were used.

Condenser

For this design the Nusselt equation was considered

sufficiently accurate for calculating the film coefficient on the water side of the condenser tubes:

$$h_i = \frac{K}{d_i}(0.023)(Re)^{0.8}(P_r)^{0.4}$$

For the ammonia side of the condenser tubes the following, generally accepted expression was used:

$$h_c = 0.725\left[\frac{\rho^2 g h_{fg} K^3}{\mu D(T_v - T_s)}\right]^{\frac{1}{4}}$$

At an assumed 80 per cent overall collector-generator efficiency, and with a solar energy input of 300 BTU/HR-FT.^{2}, a total load of 3840 BTU/HR or 64 BTU/MIN is the maximum heat rate that the condenser must reject.

With an assumed temperature difference of 10 degrees between the cooling water and the condensate, the calculated areas of heat transfer surface varied between 0.64 and 4.5 square feet, depending on the cooling water velocity.

The condenser was made up with 4 pipes, each of 1/2 inch nominal size and 48 inches long. These were symmetrically spaced inside a 3-inch pipe, giving a surface area of 3.5 square feet.

Evaporator

This unit was sized by using ranges of overall U values given by ASHRAE [32]. Depending on the water velocities and temperature differences, ranges from 50 to

190 BTU/°F-HR-FT^2 were given. Thus, at a 10 degree difference of temperature, the heat transfer areas were from 2.02 to 7.7 square feet.

The evaporator was made up with 7 lengths of 1/2-inch pipe, each 48 inches long, enclosed in a 4-inch shell. The resulting heat transfer area was 6.16 square feet.

Absorber

An approximate figure of 35 square feet of absorber area per ton of refrigeration is given by Arrowood [34]. However, the important function of the absorber is to present as large a liquid surface area as possible to absorb ammonia gas from the evaporator, with adequate provision for carrying away the heat of solution of the ammonia.

Thus, the absorber was designed for vertical operation. Two spray nozzles were placed directly opposite each other near the top, to break up the incoming weak liquor from the generator into fine droplets.

The absorber was made up from 11 three-foot lengths of 1/2-inch pipe inside a 6-inch pipe, giving a heat transfer surface area of 6.16 square feet.

Final Assembly of Complete System

All connections between the components utilized standard pipe fittings, with the exception of the special all steel unions used for final connections between units.

A special pipe compound, which expanded as it set and hardened, gave ammonia tight seals at all threaded pipe connections. There were no welded connections and there were no leaks at any connection.

Stainless steel filter screens of special design were fitted into the unions just upstream of the most critical points in the liquid flow lines. The filters were made by drawing fine mesh (1600 openings per square inch) screen into rounded cup shapes. These cups were then tightly wedged into the unions with the concave side upstream. One filter was placed upstream of the pump, and one each was placed in the unions giving access to the absorber spray nozzles.

The ammonia liquor pump was of the rotary, nylon roller type. To match the pump's capacity to the system flow requirements, a 16 to 1 speed reducer was inserted between the 1/2 horsepower drive motor and the pump shaft.

Figures 22 and 23 show the back and front views of the complete refrigeration system respectively.

The identification, flow directions, and relative positions of the units making up the system can be seen in the schematic view of Figure 24.

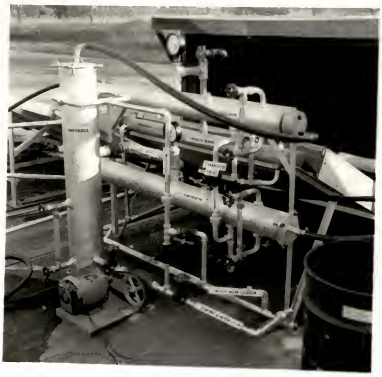

Figure 22

Figure 23

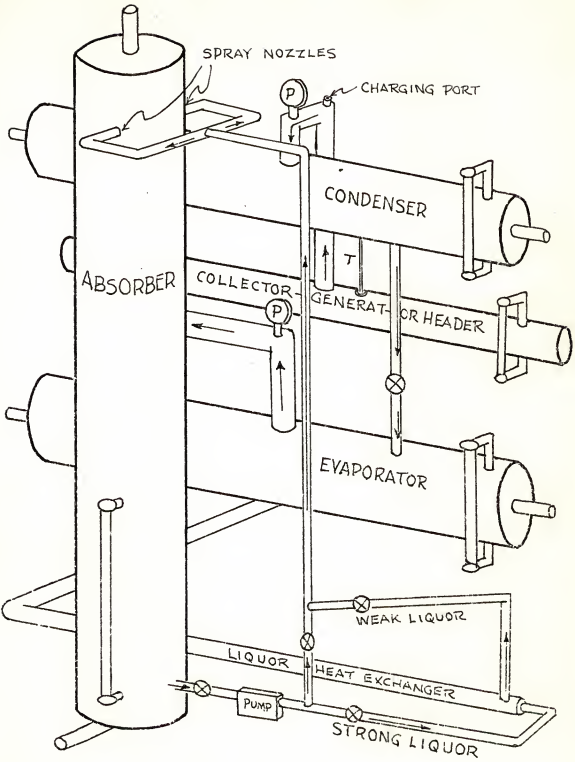
SPRAY NOZZLES
P
CHARGING PORT
CONDENSER
T
ABSORBER
COLLECTOR
P
GENERATOR HEADER
EVAPORATOR
WEAK LIQUOR
LIQUOR
HEAT EXCHANGER
PUMP
STRONG LIQUOR

Figure 24

CHAPTER VII

EXPERIMENTAL PROCEDURE

The experimental phase of this investigation was carried out in three separate series of performance tests extending over an interval of two months, each series being run at a different state of progress in the manufacture and assembly of the solar collector-generator and the associated refrigeration components. These tests were as follows:

1. Preliminary tests of the completed solar collector-generator and its enclosure as a solar energy absorber.
2. Preliminary test of the collector-generator and condenser combination as an intermittent, "one-shot" ammonia generating system.
3. Final tests of the collector-generator and all the associated refrigeration components as a complete, continuous refrigeration and air-conditioning system.

However, before any of the components were performance tested, each one was hydrostatically tested to a pressure of 300 pounds per square inch and then given a 24-hour test at approximately 30 inches of mercury vacuum. The completed systems were also tested this way again to detect any leaks in the plumbing connections. No leaks were found in any of the connections, even though there were no welded connections!

The Solar Collector-Generator Performance as a Solar Energy Absorber

To measure the solar energy collection characteristics of the collector-generator and its glass covered enclosure, the collector grid was connected to a water supply line. Cool water was fed into the lower feeder pipe of the grid and a hot water outlet connection was made at the top of the header pipe. The water flow rate was adjusted to approximate the fluid flow rates which were expected to occur later in the complete refrigeration system.

On three successive clear days, this system was operated during the hours of useable solar energy. During the 6-to 8-hour tests, the following variables were measured:

1. Water flow rate and temperature rise through the collector-generator.
2. Solar energy input intensity and angle of incidence on the plane of the inclined solar collector-generator.
3. Air temperature.

A final, no flow test was run on the fourth day to find how high a temperature could be attained by the system. During this test, only the time and temperature were recorded.

Intermittent Ammonia Generation Test

After the condenser had been connected to the

collector-generator and this combination had been pressure tested, a vacuum pump was connected to the system at the charging port and the system evacuated to approximately 30 inches of mercury and sealed off. No loss of vacuum was observed in 24 hours. Next, water was introduced into the collector-generator in an amount calculated to make the final ammonia-water mixture reach approximately to the half-full mark on the header of the collector-generator. After re-evacuating the system, liquid ammonia was charged into the system until the desired liquid level was reached. Later reweighing of the ammonia cylinder indicated that a concentration of 60 per cent ammonia by weight existed in the collector-generator.

However, temperatures along the collector-generator tubes indicated that very little mixing of the ammonia and water had occurred, due to the inclination of the tubes. This stratification effect was removed by temporarily lifting the lower end of the collector-generator to a level higher than the header. This procedure, repeated at about 1-hour intervals to allow the heat of solution to dissipate, finally brought the pressure of the mixture down to a level indicating a mixture of about 60 per cent concentration.

A 5-hour performance test was run on a clear day to evaluate the static, ammonia generating characteristics of the solar collector-generator. The following variables

were recorded at 15-minute intervals:

1. Generator header liquid level and temperature.
2. Condenser pressure, temperature, and liquid level.
3. Solar intensity and angle of incidence on the plane of the collector-generator.

Final Performance Tests of the Collector-Generator in the Complete Refrigeration System

After the collector-generator, condenser, evaporator, absorber, liquid heat exchanger, and liquor pump had been connected, and pressure and vacuum tested, the system was charged with approximately a 60 per cent ammonia-water mixture.

Various preliminary practice tests of the pump and pump motor indicated that the 1/3-horsepower electric motor did not have the torque characteristics to match the pump torque required for the extremely low liquid flow rates desired in the system. This difficulty was not resolved until the final test run was made, at which time the pump driving system was replaced by a 1/2-horsepower motor acting through a 16 to 1, double pulley, speed reducing mechanism.

The season being mid-winter, the occurrence of clear days was rather infrequent. So, an artificial heat source consisting of a 3 x 3 grid of 750 watt radiation heat lamps was arranged to simulate the radiant heat input

from the sun. This array of lamps was set up at a distance of 2 feet from the collector-generator, with the cover glass removed and the entire system covered to reduce convection and radiation losses. At the conditions prevailing on the day of the test, the generator temperature did not quite reach 110°F after several hours' operation, so this method of heating was not pursued further.

Later, after solving some minor pump leakage problems, the system was tested on a fairly clear, warm day. During this final test, the following variables were recorded at 20-minute intervals:

1. Collector-generator pressure and temperature rise.
2. Condenser cooling water flow rate and temperature rise.
3. a. Evaporator pressure and liquid level.
   b. Chilled water flow rate and temperature drop.
4. Absorber cooling water temperature rise.
5. Solar energy intensity and angle of incidence on the plane of the collector-generator.
6. Air temperature.

Since the cooling water circuit of the absorber was in series with the condenser cooling circuit, one flow rate measurement sufficed for both. The flow rates were measured by weighing the water accumulation per unit time in a bucket.

To approximate steady conditions in the system, the

expansion valve was kept slightly cracked during the test. By careful adjustment of the control valves in the ammonia liquor flow lines, an almost steady flow condition was achieved in the liquor flow to and from the generator. However, due to the pump's over-capacity, it was difficult to maintain a steady liquid level in the absorber, this level varying $\pm$ 3 inches from a 6-inch average level. To provide good absorption, the by-pass valve on the pump output was adjusted to give continuous recirculation of fluid through the absorber spray nozzles.

A gravity operated water recirculation system was used to provide the low flow rates of chilled water through the evaporator.

CHAPTER VIII

DATA AND RESULTS

Collector-Generator Water Heating Test Runs 1, 2, 3, and 4

This series of tests to determine the solar energy collection characteristics of the collector-generator was run on October 27, 28, 29, and 30, 1966. The conditions during the test runs were ideal. The solar intensity, solar incidence angles and ambient temperatures existing during this period resulted in the collection of good, consistent data. The sky was perfectly clear on each of the test days.

The test on October 27th was only a practice run, primarily to check out the instrumentation and flow controls. Although instrument readings were made, the results were not considered pertinent to this investigation.

Calibration of Condenser and Evaporator Volumes

Since it was necessary to read the ammonia volumes directly in all the subsequent tests, the sight glasses on the condenser and evaporator were calibrated in terms of centimeter scale readings versus cubic feet of liquid ammonia volume in the particular unit.

This calibration was done after the units had been

permanently fastened in position on a steel rack. Measured volumes of water were poured into the units and the liquid level reading on the sight glass noted for each increment of volume added. These two calibration curves are included in the Appendix.

Intermittent Ammonia Generation Tests
Runs 5 and 6

The first of the series of two tests of the collector-generator and condenser alone as an intermittent ammonia generating system was started on the morning of November 19, 1966. After about one hour of operation it was observed that the pressures and temperatures of the generator were following the saturation curve for pure liquid ammonia. This indicated that a layer of pure ammonia liquid was stratified in the upper part of the collector-generator header and tubes. It was decided to postpone further testing until the water-ammonia charge in the collector-generator had been thoroughly mixed.

On November 22nd, a 5-hour performance test was run under ideal conditions. There were no clouds in view, the ambient temperature remained in the middle sixties, and there was very little air movement.

Continuous Ammonia Generation Tests
Runs 7 and 8

The test using an artificial source of radiant heat was run on January 4, 1967. Although the generator temperature reached was moderate, the results were considered quite significant.

The final test was run on January 7, 1967, under satisfactory conditions. By mid-morning most of the sky was clear and the test proceded through a 7-hour period. Ambient temperatures climbed into the middle seventies, and there were a few, very light breezes.

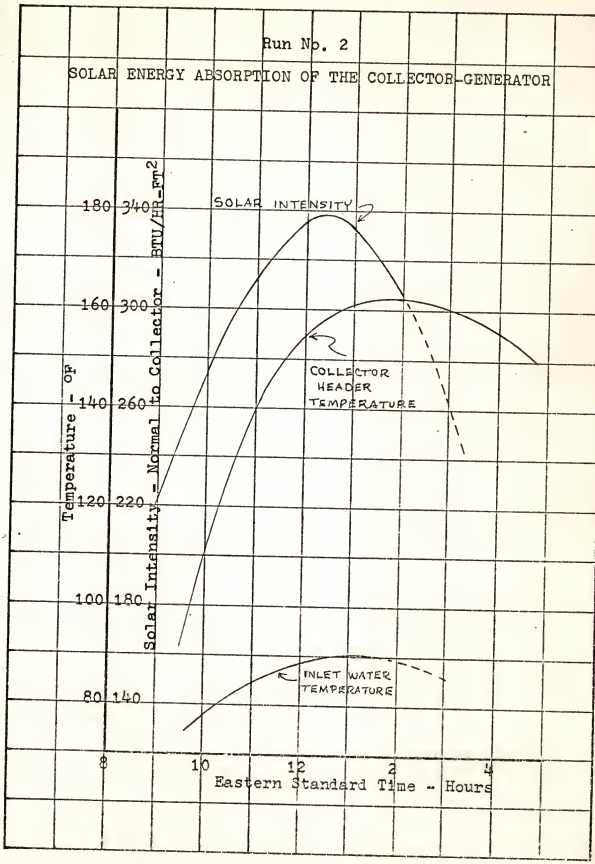
Run No. 2
SOLAR ENERGY ABSORPTION OF THE COLLECTOR-GENERATOR
Solar Intensity - Normal to Collector - BTU/HR-FT2
Temperature OF
180 340
160 300
140 260
120 220
100 180
80 140
SOLAR INTENSITY
COLLECTOR HEADER TEMPERATURE
INLET WATER TEMPERATURE
8
10
12
2
4
Eastern Standard Time - Hours

Figure 25

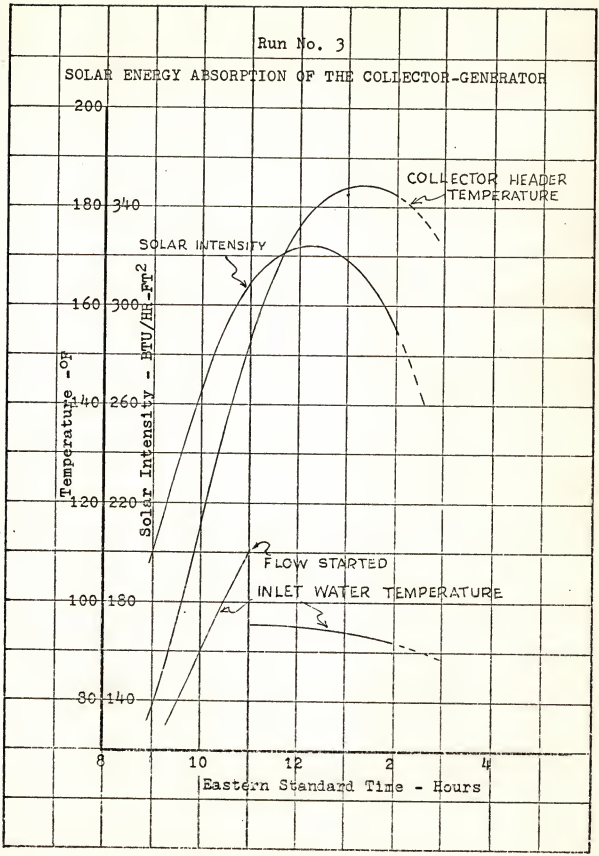
Run No. 3
SOLAR ENERGY ABSORPTION OF THE COLLECTOR-GENERATOR
200
180
160
140
120
100
80
Temperature - °F
340
300
260
220
180
140
Solar Intensity - BTU/Hr.-Ft.²
SOLAR INTENSITY
COLLECTOR HEADER TEMPERATURE
FLOW STARTED
INLET WATER TEMPERATURE
8
10
12
2
4
Eastern Standard Time - Hours

Figure 26

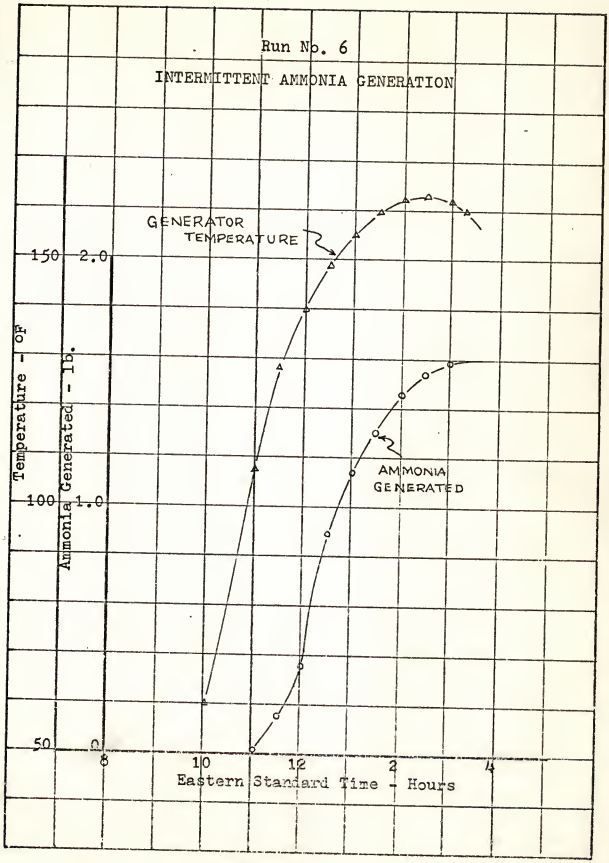
Run No. 6
INTERMITTENT AMMONIA GENERATION
GENERATOR TEMPERATURE
AMMONIA GENERATED
Temperature - °F
Ammonia Generated - lb.
150
100
50
2.0
1.0
0
8
10
12
2
4
Eastern Standard Time - Hours

Figure 27

Table 1 Observed Data, Run No. 7, January 4, 1967

TIME E.S.T	GENERATOR		CONDENSER				EVAPORATOR					ABSORBER		
			WATER			NH_3	WATER				NH_3	WATER		NH_3 IN
P.M.	°F	PSIG	IN °F	OUT °F	LB/MIN	CM.	PSIG	IN °F	OUT °F	LB/MIN	CM.	IN °F	OUT °F	EVAP. LB
3:45	78	55	62	62	17.2	4.9	57				4.6	62	62	1.011
4:00	84	67	64.5	64.5		5.0	54	62	61.5		4.6	64.5	64.5	1.011
:15	94	79	66.5	66.5		3.5	67	61	64		5.9	66.5	66.5	2.39
:30	98	83	67	67.2	17.1	3.5	76	60.5	65	3.6	6.1	67	67	2.54
:45	103	84	67.2	68.5		3.5	86	60.5	61.5		6.2	67.5	67	2.70
5:00	106	86	67	68.5		3.5	92	60.5	60	2.1	6.4	68	67	2.93
:15	109	89	67	67.5		3.5	92							
:30	107	84	67	67.2		3.5	88	60.2	58.5	2.1	6.6	67.5	67	3.20
:45	106	86	67	67		3.6	90	60.5	59	2.2	7.1	67.5	67	3.77
6:00	104	82	66.5	67	17.3	3.6	85	59.5	57		7.3	66.5	66.5	3.93

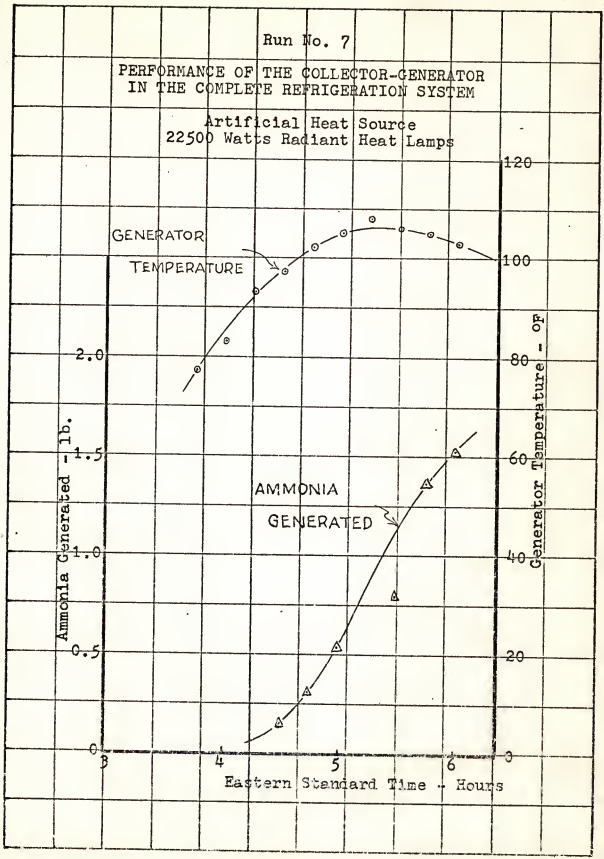
Run No. 7
PERFORMANCE OF THE COLLECTOR-GENERATOR
IN THE COMPLETE REFRIGERATION SYSTEM
Artificial Heat Source
22500 Watts Radiant Heat Lamps
GENERATOR
TEMPERATURE
AMMONIA
GENERATED
Ammonia Generated - lb.
Generator Temperature - °F
Eastern Standard Time - Hours
0
0.5
1.0
1.5
2.0
20
40
60
80
100
120
3
4
5
6

Figure 28

Table 2 Observed Data, Run No. 8, January 7, 1967

HOUR	SUN	GENERATOR		COND. WATER			COND.	EVAPORATOR				EVAP	ABSORBER H_2O		NH_3 IN	NH_3 TO
E.S.T.	M.V.	°F	PSIG	IN °F	OUT °F	LB/MIN	NH_3 CM.	PSIG	IN °F	OUT °F	LB/MIN	NH_3 CM	IN °F	OUT °F	EVAP-LB	ABS.-LB
9:30		57	59	59	57		5.3	59	58	59		5.8	59	59		
10:00		72	70	60	59	14.2	3.5	59	57.5	59		6.5	60	60		
:20		78	73	61	60		3.6	70	58	58.5	3.6	6.5	60	61		
:40		90	70	62	62		3.5	67	59	59		6.5	63	62		
11:00		110	95	64	65		3.6	90	58.5	58		6.5	63	63.5	0.00	0.069
:20		122	97	67	67		3.6	93	58.5	57.5	4.0	6.7	65	67	0.22	0.22
:40	2.9	134	99	69	70		3.5	94	58.5	58		7.1	68	69	0.65	0.30
12:00		140	100	70	72	14.5	3.5	94	59	58		7.4	70	72	0.90	0.45
:20	3.1	144	103	70	73		3.5	95	59.5	58	3.5	7.8	69	72.5	1.12	0.66
1:45		140	100	71	72		3.5	93	62	60.5		8.0	70	71	1.35	0.87
2:00		145	103	72	74	13.9	3.4	94	62	60.5	3.7	8.2	69	72	1.54	1.08
:20		138	101	73	75		3.4	94	61	59.4		8.5	68	73	1.77	1.31
:40	2.7	133	99	73	77		3.5	96	61.2	59.1		8.7	70	73.5	2.10	1.61
3:00		131	101	75	79	14.7	3.5	95	61	58.5	4.1	9.0	71	75	2.43	1.93
:20	2.5	130	99	75	79		3.5	90	60.8	58		9.3	70	75	2.91	2.37
:40	2.4	129	95	73	78		3.3	90	60	57.7		9.8	69	73	3.54	2.73
4:00		127	99	72	76	14.1	3.3	92	59	57		10.0	68	72	3.78	3.05
:20		114	93	72	76		3.5	88	58	56.5	4.1	10.2	68	72	3.85	3.29
:30		110	95				3.8	91	58	56.2		10.3				

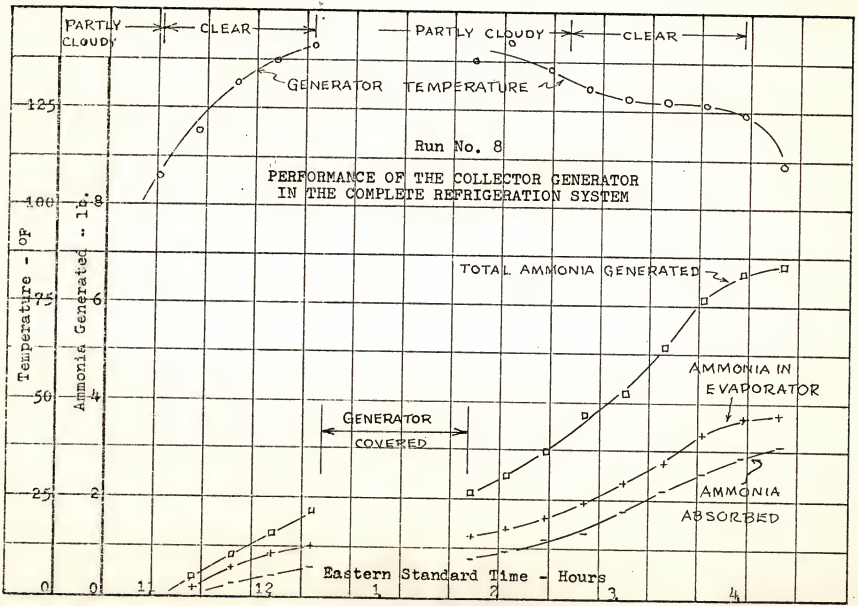
PARTLY CLOUDY
CLEAR
PARTLY CLOUDY
CLEAR
GENERATOR TEMPERATURE
Run No. 8
PERFORMANCE OF THE COLLECTOR GENERATOR
IN THE COMPLETE REFRIGERATION SYSTEM
TOTAL AMMONIA GENERATED
AMMONIA IN EVAPORATOR
GENERATOR COVERED
AMMONIA ABSORBED
Temperature - °F
Ammonia Generated - lb.
125
100
75
50
25
0
8
6
4
2
0
11
12
1
2
3
4
Eastern Standard Time - Hours

Figure 29

CHAPTER IX

DISCUSSION AND EVALUATION OF RESULTS

The primary objective of this investigation was fully met in eliminating the heat loss that normally would occur between the solar collector and the generator when these two were separate units. The combining of the solar collector and the generator into one unit removed the need for fluid transport between the collector and the generator, along with its resultant heat loss.

At several points between the various series of experimental investigations it was necessary to open the pressurized system and drain out the refrigerant. During each of these operations it was observed that the liquid ammonia in the condenser and in the evaporator boiled away completely, leaving no water residue. This was direct evidence that complete separation of the water and the ammonia had occurred at the large liquid surface area provided in the collector-generator header. This also verified the theoretical prediction that the steady state vapor generation rate would be low enough to prevent any boil-over of the ammonia due to vapor choking or slugging in the collector-generator tubes.

Besides the elimination of the heat loss mentioned above, there were other advantages resulting from the com-

bining of the collector and the generator. Several of these advantages were brought out in the first series of investigations of the solar energy absorption capabilities of the collector generator alone. The results of this series indicated good collection efficiency, relatively low heat storage capacity for the collector-generator, and gave a measure of the resulting thermal lag of the unit and its liquid content.

This heat storage effect is due to the total heat capacity of the system. This heat capacity is the sum of the products of the masses of the various materials comprising the system times their respective specific heats. For example, the steel in the collector-generator grid weighed 158.2 pounds. At the operating level, the liquid contained in the generator weighs 27.2 pounds. Thus, with a specific heat of 0.12 BTU/LB^{o}F for the steel and 1.0 BTU/LB^{o}F for the water, the heat capacity of the collector-generator and its contents is 46 BTU/^{o}F.

A heat balance for the collector-generator can be evaluated thus:

$$Q_{INPUT} = Q_{STORED} + Q_{OUTPUT} + Q_{LOSSES} .$$

Selecting a linear portion of the curves for run number 2 (9:00 a.m. to 10:00 a.m.) and using arithmetic mean values, the heat balance becomes:

$$(16\ FT^2)(251\ \frac{BTU}{HR\ FT^2}) = 1600\ \frac{BTU}{HR} + 511\ \frac{BTU}{HR} + Q_{LOSSES}.$$

These figures indicate a collection efficiency of about 50 percent. The loss to surroundings could have been reduced by use of more insulation in the collector-generator enclosure.

The relatively low heat capacity of the collector-generator is a definite advantage if it is desired to reach ammonia generating temperatures quickly. On the other hand, if it is desired to have ammonia generation occur for a considerable time after the solar energy input has diminished, as is the case in late afternoon, then a collector-generator with a larger heat capacity would be needed, since the stored heat would generate ammonia until the collector-generator temperatures dropped below the ammonia generation temperature.

Another characteristic of the collector-generator is evident in the performance curves of runs number 2 and number 3. Note that, for both runs, there was approximately a 1-hour interval after solar noon (peak solar intensity) before the collector-generator reached its peak temperature. This delay is the effect of a system characteristic called the thermal time constant, which is a function not only of the collector-generator's heat

storage capacity, but also of its heat loss rate. If this heat loss rate under steady conditions is expressed as the thermal resistance of the collector-generator's enclosure, then the product of thermal capacity C and thermal resistance R is the thermal time constant for the collector-generator. This is directly analogous to the time constant in an electric circuit, RC, where R and C are the electrical resistance and electrical capacities in the circuit.

Thus the results of the first series of experimental runs predict a relatively short warm-up time for the subsequent ammonia generating tests of the collector-generator. In addition to this, the collector-generator temperatures reached in these runs indicate potential ammonia generating temperatures in the range of 185 to 190° F, thus allowing the use of lower ammonia concentrations in the generator with resulting lower generator and condenser pressures. This, in turn, should permit less rugged construction and a still further reduction in thermal lag and in the fixed cost.

In all the subsequent runs where the ammonia generating capabilities were tested, the time from cold start to first ammonia production was between 1-1/4 and 1-1/2 hours, bearing out the prediction of fast warm-up time.

The results of run number 7 point out an unique advantage of the flat plate type collector-generator as compared to a concentrating type collector. The concentrating type collector can absorb only the specular component of the incoming solar energy, rejecting the diffuse energy. Thus, on a hazy day, when the diffuse portion of available solar energy may comprise about 90 percent of the total energy, the flat plate solar collector-generator can easily maintain a temperature of 110°F and better where the concentrating type collector would remain cold. Note that, in run number 7, at a generator temperature of about 110°F, there is a substantial output of ammonia after the 1-hour warm-up period. Thus, the results of run number 7 indicate that the solar collector-generator is fully capable of maintaining a substantial ammonia production rate even on hazy or cloudy days.

The results of the final test run (number 8) are presented in terms of total ammonia output so as to average out the transient effects that occurred during the test.

In order to arrive at a better estimate of the potential ammonia generating capacity of the solar collector-generator at a time of year when air-conditioning is needed, the results of this final test will be correlated with conditions existing in Gainesville, Florida

during early July.

Correlation Analysis

Gainesville, Florida is at latitude 29°42'N and longitude 82°16'W. For convenience, this latitude will be rounded off to 30.0°. Since the plane of the solar collector-generator is inclined 30° above the horizontal and faces due south, the hourly solar intensity on such a surface was computed for a location at 30° north latitude. These values were calculated for a clear day in early January and for a clear day in early July. The resulting curves are shown in Figure 30 .

The summer air-conditioning design conditions for Gainesville, Florida [35] call for a dry bulb temperature ranging from 89 to 96°F. The daily average insolation on a horizontal surface at Gainesville, Florida is 1011 BTU/Ft.^{2} in January and 1823 BTU/Ft.^{2} in July, according to weather bureau records [35] . These relations can be compared best when seen side by side in a table:

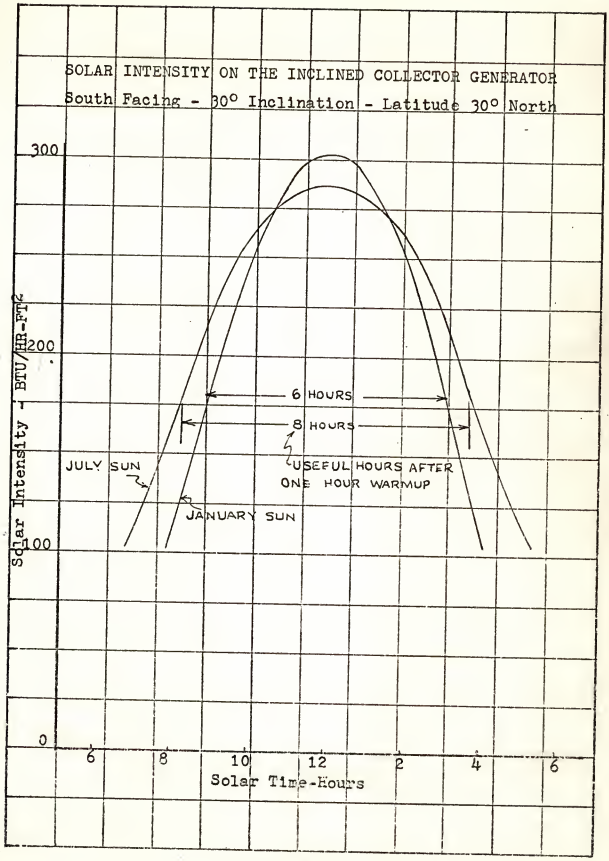
SOLAR INTENSITY ON THE INCLINED COLLECTOR GENERATOR
South Facing - 30° Inclination - Latitude 30° North
300
200
100
0
Solar Intensity - BTU/HR-FT²
6 HOURS
8 HOURS
USEFUL HOURS AFTER ONE HOUR WARMUP
JULY SUN
JANUARY SUN
6
8
10
12
2
4
6
Solar Time-Hours

Figure 30

Table 3 Solar Energy Correlation

Item	January Conditions	July Conditions
Ambient Temperature	75°	90°
Average Daily Insolation	1011 $\frac{BTU}{HR - FT^2}$	1823 $\frac{BTU}{HR - FT^2}$
Total Hours Useful for Collection	6 Hours	8 Hours
ΔT For Collector Losses	$145 - 75 = 70^{\circ}$	$145 - 90 = 55^{\circ}$

If it is assumed that most of the collector losses are other than radiation losses, then these losses will be proportional to the difference in the temperatures of the generator and of the surroundings. The percent decrease in losses in July would be 78 percent or, the increase in output would be 22 percent.

The percent increase of output due to longer day length will be proportional to the increase in the number of hours of useful collection, or a 33 percent increase.

Thus, the collector-generator should, under July conditions, produce 55 percent more than it did under the actual test conditions.

Then, since 7.14 pounds of ammonia were generated during the test, the July output should be 11.0 pounds of ammonia per day. At an approximate heat of vaporization of 500 BTU/Lb. this ammonia output of the collector-generator

would be equivalent to 5500 BTU of cooling or refrigeration.

In terms of ice production, this small 4 x 4 foot solar collector-generator could produce 30 pounds of ice daily from 75°F water, or about 2 pounds of ice per day for each square foot of collector-generator frontal surface.

CHAPTER X

CONCLUSIONS

Giving due consideration to the significant results of this investigation, the following conclusions may be drawn:

1. The successful combining of the flat plate solar energy collector and the ammonia generator into a single unit has been shown to be technically feasible.

2. The combining of the two units into a single collector-generator has eliminated the heat loss formerly occurring between the solar collector and the ammonia generator.

3. The combined collector-generator developed in this investigation has a low heat capacity per unit area and, as a result, can be heated to a useful generating temperature in a relatively short time (about one hour for the unit tested).

4. This flat plate type solar collector has proven itself capable of generating substantial amounts of ammonia even on cloudy days when only diffuse solar energy is available.

5. The collector-generator tested is capable of generating the equivalent of 30 pounds of ice per day with only a 4 by 4 foot frontal area.

BIBLIOGRAPHY

1. Daniels, F., Direct Use of Solar Energy, Yale University Press, New Haven, 1964,226.

2. Kapur, J. C., United Nations Conference on New Sources of Energy, Gen. 8, Rome, 1961.

3. Green, W. P., "The Utilization of Solar Energy for Air-Conditioning and Refrigeration in Florida," Master's thesis, College of Engineering, University of Florida, 1936.

4. Chari, R. K., "An Investigation of the Use of Solar Energy for Absorption Refrigeration," Master's thesis, College of Engineering, University of Florida, 1958.

5. Eisenstadt, M. M., "An Investigation of an Ammonia-Water Absorption System for Solar Air-Conditioning," Master's thesis, College of Engineering, University of Florida, 1959.

6. Lopez, L., "A Continuous Absorption Refrigeration System Driven by Flat Plate Solar Collectors," Master's thesis, College of Engineering, University of Florida, 1962.

7. Polifka, R. W., "Operation and Performance of the University of Florida Solar Air-Conditioning System," Master's thesis, College of Engineering, University of Florida, 1964.

8. Trombe, F., and Foex, M., "The Production of Cold by Means of Solar Radiation," Journal of Solar Energy Science and Engineering, 1, January 1957.

9. Williams, D., et al., "Intermittent Absorption Cooling Systems with Solar Regeneration," Refrigeration Engineering, 66, 33, November, 1958.

10. Kapur, J. C., "A Report on the Utilization of Solar Energy for Refrigeration and Air-Conditioning Applications," Solar Energy, No. 4, 1960.

11. Tabor, H., "Use of Solar Energy for Cooling Purposes," United Nations Conference on New Sources of Energy, E 35 Gr-518, Rome, 1961.

12. Chinappa, J., "Performance of an Intermittent Refrigerator Operated by a Flat Plate Collector," Solar Energy, No. 6, 1962.

13. Chinappa, J., "Experimental Study of the Intermittent Vapor Absorption Refrigeration Cycle Employing the Refrigerant-Absorption Systems of Ammonia-Water, and Ammonia-Lithium Nitrate," Solar Energy, No. 5, 1961.

14. Chung, R., Lof, G., and Duffie, J., "Experimental Study of a Lithium Bromide-Water Absorption Air-Conditioner for Solar Operation," A.S.M.E. Paper 62-WA-347,1962.

15. Threlkeld, J. L., Thermal Environmental Engineering, Prentice-Hall, Englewood Cliffs, 1962, 351.

16. Parmalee, G. V., "Transmission of Solar Radiation Through Flat Glass," ASHVE Trans., 51, 317, 1945.

17. ASHVE Trans., 51, 332, 1946.

18. Valasek, J., Introduction to Theoretical and Experimental Optics, Wiley, 1949, 199-201.

19. Bliss, R. W., "The Derivation of Several Plate Efficiency Factors Useful in the Design of Flat-Plate Solar Heat Collectors," Solar Energy III, 4, 55-64, December 1959.

20. Kutatedeladze, S. S., Fundamentals of Heat Transfer, Academic Press, New York, 1963.

21. Rohsenow, W. M., and Clark, J. A., "A Study of the Mechanism of Boiling Heat Transfer," ASME Trans., 73, 609-620, 1951.

22. Rayliegh, Lord, Philosophy Magazine, 34, 94, 1917.

23. Fritz, W., and Ende, W., Phys. Z., 37, 391, 1936.

24. Zuber, N., "Nucleate Boiling," International Journal of Mass and Heat Transfer, 6, 53-78, 1963.

25. Fritz, W., Phys. Z.,36, 379, 1935.

26. Stokes, G. G., Mathematics and Physics Papers, Cambridge University Press, London, 1880.

27. Allen, H. S., Philosophy Magazine, 50, 323, 1900.

28. Robinson, J. V., Journal of Physical and Colloidal Chemistry, 51, 431, 1947.

29. Farber, E. A., and Scorah, R. L., ASME Trans., 70, 4, 369-384, 1948.

30. Kruger, R. A., and Rohsenaw, W. M., "Film Boiling Inside Horizontal Tubes," Proceedings of the International Heat Transfer Conference, 5, 60-68, 1966.

31. Sachs, P., and Long, R. A. K., "A Correlation for Heat Transfer in Stratified Two-Phase Flow with Vaporization," International Journal of Mass and Heat Transfer, 2, 222-230, 1961.

32. ASHRAE Guide and Data Book; Fundamentals and Equipment for 1965 and 1966, American Society of Heating, Refrigeration, and Air-Conditioning Engineers, Inc.

33. Jakob, M., Heat Transfer, I, Wiley, New York, 1957.

34. Arrowood, M. W., Refrigeration, American Technical Society, Chicago, 1917.

35. Strock, C., and Koral, R. L., Handbook of Air-Conditioning, Heating and Ventilating, Industrial Press, New York, 1965.

APPENDIX

Table 4 Observed Data, Run No. 2, October 28, 1966

HOUR	WATER			AIR	SUN		
C.S.T.	IN °F	OUT °F	lb/MIN	°F	MY	Θ	
8:30		62					
9:00		75		61	2.32	50°	
:15	74.5	87		62	2.49	45	
:30	75	95.5	0.50	62.8	2.61	43	
:45	79	104.5		64.2	2.75	39	
10:00	79.8	113	0.53	66.6	2.80	36	
:15	82	120	0.45	66.3	3.05	32	
:30	83	127		67.4	3.06	29	
:45	84	133	0.50	68	3.24	26	
11:00	86	138	0.43	68.4	3.29	24	
:15	87.5	143	0.49	68.5	3.40	20	
:30	88	147.5	0.48	69.2	3.41	17.5	
:45	89	151.5	0.44	69.6	3.42	16	
12:00	89.5	155	0.49	69	3.45	16	
:15	90	158.5	0.46	70.3	3.48	15	← SOLAR NOON
THERMOMETER BROKEN							
3:45	82.5	142		75	1.9	56	
4:00	81	139	0.41	73.2	1.67	60	
:15	80	134	0.43	73.8	1.40	64	
:30	78	129.5	0.38	74	1.22		

Table 5 Observed Data, Run No. 3, October 29, 1966

HOUR	WATER			AIR	SUN	
C.S.T.	IN °F	OUT °F	LB/MIN	°F	MV	θ
8:15	61	58	↑	58.5		
9:00	70	78		63.2	2.13	49°
:15	74	88		65.6	2.27	46
:30	80	97.5		68	2.47	43
:45	85	107	NO FLOW	69.4	2.61	39
10:00	91.5	117		70.8	2.76	34
:15	98	126		71.7	2.84	31.5
:30	102	135		72.8	3.02	29
:45	107	144	↓	74	3.08	26
11:00	110	152		74	3.21	23
:15	95	159	0.17	75	3.24	20
:30	89	165.5	0.35	75.8	3.30	17.5
:45	94	171			3.30	15
12:00	95	175.5	0.293	77.2	3.31	15
:15	96	179.5		76.2	3.35	15
:30	94.5	182.5		76	3.41	15.5
:45	96	185.0		77.7	3.24	17
1:00	94.5	186	0.319	77.2	3.23	
:15	95.5	186		80.1	3.20	22
:30	94	186.5		79	3.16	25.5
:45	93.5	186		79.8	3.04	28.5
2:00	92.5	186	0.265	79.6	3.01	
:15	92	184.5		79.9	2.83	35

Table 6 Observed Data, Run No. 4, October 30, 1966

C.S.T.	WATER INLET °F	HEADER °F
10:00	71°	71°
2:15	130	192
:30	130	192.7
:45	130	191.8
3:00	130	190.5
:15	130	189

Table 7 Observed Data, Run No. 6, November 22, 1966

HOUR	SUN		AIR	GENERATOR		CONDENSER		NH_3
E.S.T.	MV.	θ	°F	°F	PSIG	°F	LEVEL cm.	lb.
10:00	2.68	36°	56	60	58	59	4.00	0.302
11:00	3.01	28.5	58.4	108	95	67	4.05	0.310
:15	3.08	25.5	60.4	119	104	69	4.10	0.322
:30	3.14	23.5	60	128	129	71	4.2	0.453
:45	3.16	22	60	134	141	72	4.3	0.528
12:00	3.22	21	62.5	140	152	74.5	4.5	0.660
:15	3.22	20	62	145	160	76.5	5.0	0.965
:30	3.26	20.5	63	149	165	76.8	5.5	1.190
:45	3.21	21	63.4	152	171	76.6	5.8	1.32
1:00	3.19	22	62.8	155	174	76	6.0	1.44
:15	3.18	23.5	62.2	158	178	75.5	6.1	1.47
:30	3.09	26	64.2	159.5	181	75.5	6.2	1.58
:45	3.05	29	64.7	161.5	184	74.7	6.3	1.62
2:00	2.89	31	62	162.5	184	74	6.4	1.74
:15	2.80	34	62.4	163	185	73	6.5	1.85
:30	2.68	37.5	62	163.5	186	71.6	6.52	1.85
:45	2.48	41	62.6	163	185	70.7	6.55	1.89
3:00	2.29	43.5	62.2	161.5	184	69.6	6.55	1.89
:15	2.28	46	61.5	159.5	180	68.5	6.6	1.91

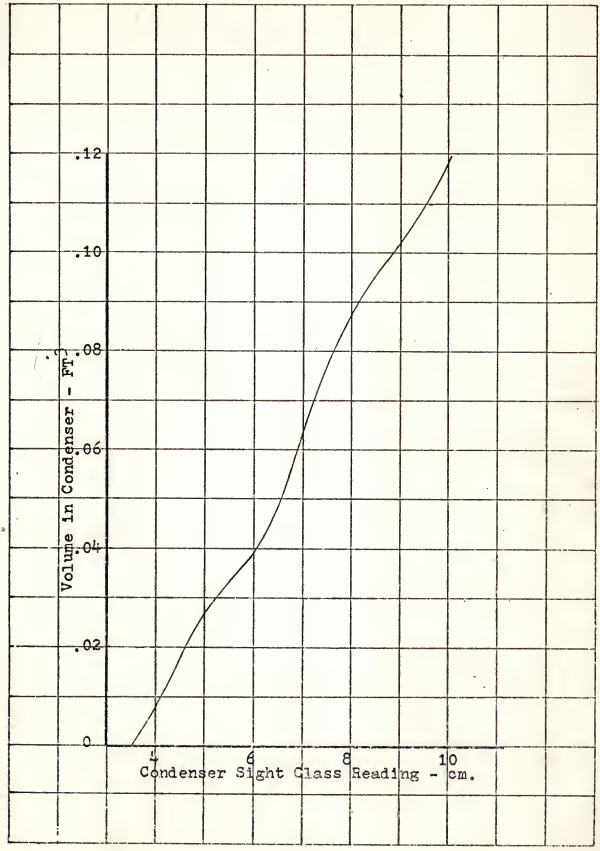
.12
.10
.08
.06
.04
.02
0
Volume in Condenser - Ft.³
4
6
8
10
Condenser Sight Glass Reading - cm.

Figure 31

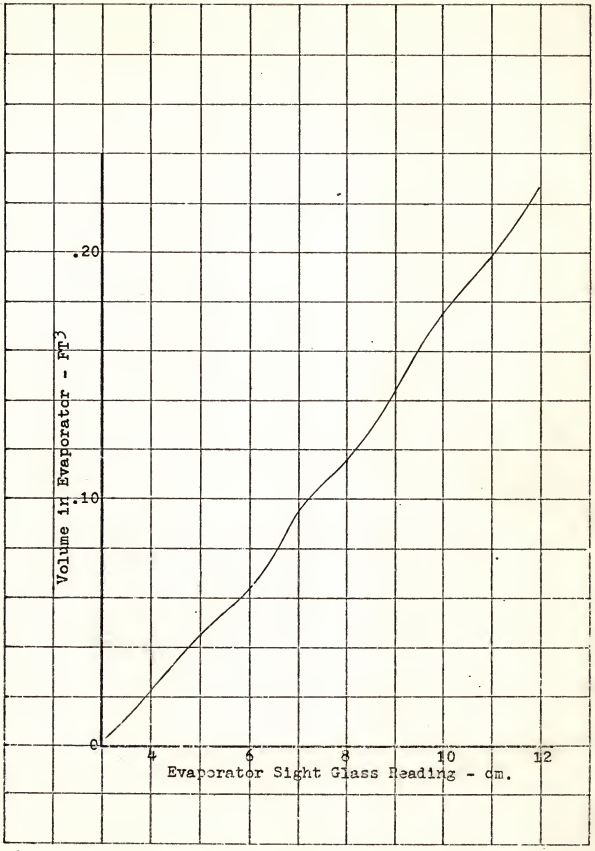
.20
.10
0
Volume in Evaporator - FT³
4
6
8
10
12
Evaporator Sight Glass Reading - cm.

Figure 32

BIOGRAPHICAL SKETCH

Gordon Lee Moore was born July 23, 1916, at Independence, Missouri. There he graduated in June, 1934 from William Chrisman High School. In the intervening years before coming to the University of Missouri at Columbia, he was employed as a commercial photographer, as a photo-engraver, as a news photographer, and as a taxi operator. One year was spent in attending night school at Kansas City Junior College. His subsequent attendance at the University of Missouri was interrupted by military service in the Army Air Force from January 6, 1943 until February 11, 1946.

Returning to the University of Missouri, he received the degree of Bachelor of Science in Mechanical Engineering in June of 1949. At this time he began a career of study and teaching. He was awarded the degree of Master of Science in Mechanical Engineering at the University of Missouri in June, 1953.

In the fall of 1964 he began his graduate work toward the degree of Doctor of Philosophy at the University of Florida. During the 1964-65 school year he worked as a Graduate Assistant assigned to the Solar Energy Laboratory. The work involved in this project led to the joint publication of a scientific paper by the student and Professor

Clark W. Pennington. In the 1965-66 school year he was appointed a Research Associate in the Mechanical Engineering Department of the University of Florida.

Upon completion of the requirements for the doctoral degree, he will return to full-time teaching at the University of Missouri at Columbia in the Department of Mechanical Engineering, where his present rank is Associate Professor.

Gordon Lee Moore is single and is a member of the American Society of Mechanical Engineers, American Society of Heating, Refrigerating, and Air-Conditioning Engineers, the Solar Energy Society, Pi Tau Sigma, Tau Beta Pi, and Sigma Xi.

This dissertation was prepared under the direction of the chairman of the candidate's supervisory committee and has been approved by all members of that committee. It was submitted to the Dean of the College of Engineering and to the Graduate Council, and was approved as partial fulfillment of the requirements for the degree of Doctor of Philosophy.

August, 1967

Dean, College of Engineering

Dean, Graduate School

Supervisory Committee:

Chairman